Finite temperature magnetism in dilute magnetic semiconductors

Materials design for semiconductor spintronics

ISIR, Osaka Univ.,
IFF, FZ-Juelich
K. Sato, T. Fukushima,
H. Katayama-Yoshida and P. H. Dederichs

Ab initio simulation at finite temperature

Diffusion of
Cu in Si

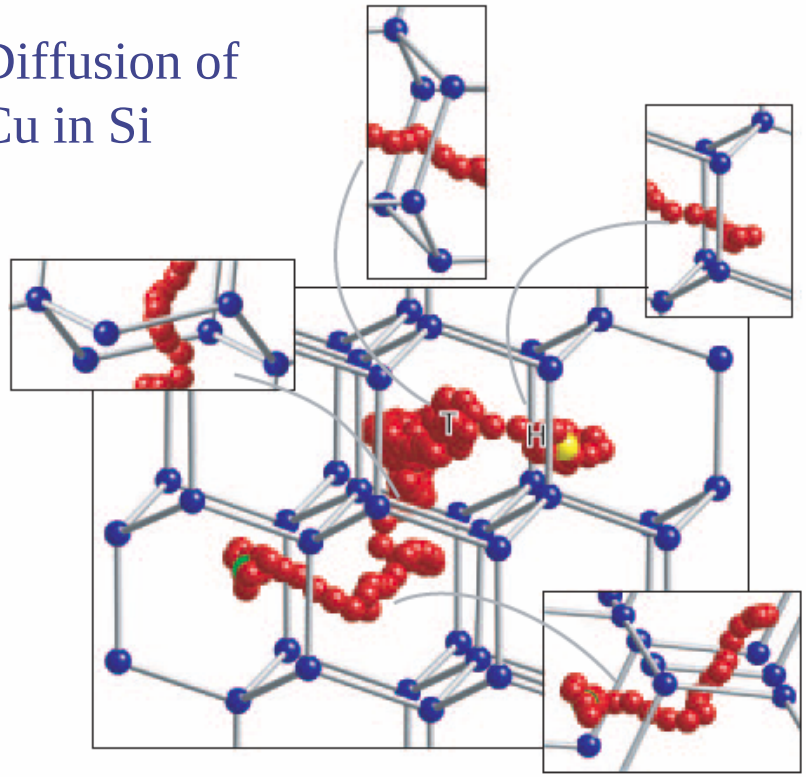

Fig. 3. Trajectory of Cu atom in MD simulation at $T = 1120$ K. Over a period of 9.7 ps, the Cu atom (red and large sphere) migrates from the initial position indicated by the thin gray (yellow) sphere, to the final position indicated by the thick gray (green) sphere.

- Ab initio Molecular dynamics
- Electronic structure calculation + molecular dynamics simulation
- Atomic motion at finite temperature
- Successfully applied to
  - Lattice relaxation
  - Phase transformation
  - Impurity diffusion
  - Chemical reaction

⇒ Ab initio spin dynamics?

K. Shirai, *et. al.*, Jpn. J. Appl. Phys. **44** (2005) 7760.

Simulation for finite temperature magnetism

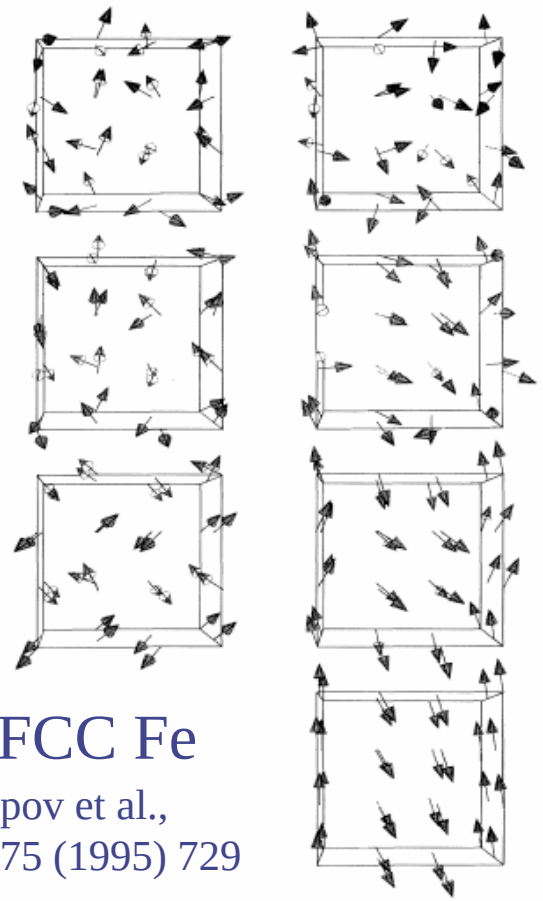

FCC Fe

Antropov et al.,
PRL 75 (1995) 729

FIG. 1. The left column shows the evolution of spins in a 32-atom cell of fcc Fe with $a = 3.59$ Å. Top, the starting random configuration; middle, after 75 steps; bottom, after 200 steps. This last configuration is close to a 3**k** structure, the minimum-energy structure allowed by the simulation (no SS allowed). The right column is similar, but for $a = 3.73$ Å. Spin configurations after 0, 20, 75, and 220 steps are shown, the last being close to the ↑↑↓↓ structure.

- Ab initio spin dynamics
- FCC Fe
  - Supercell (32 atoms)
  - 3k spin structure (a=3.59Å)
  - ↑↑↓↓structure (a=3.73Å)
- Computationally demanding

Practical method

① Disordered local moment (DLM) state by using coherent potential approximation (CPA)

② Mapping on Heisenberg model

Coherent potential approximation

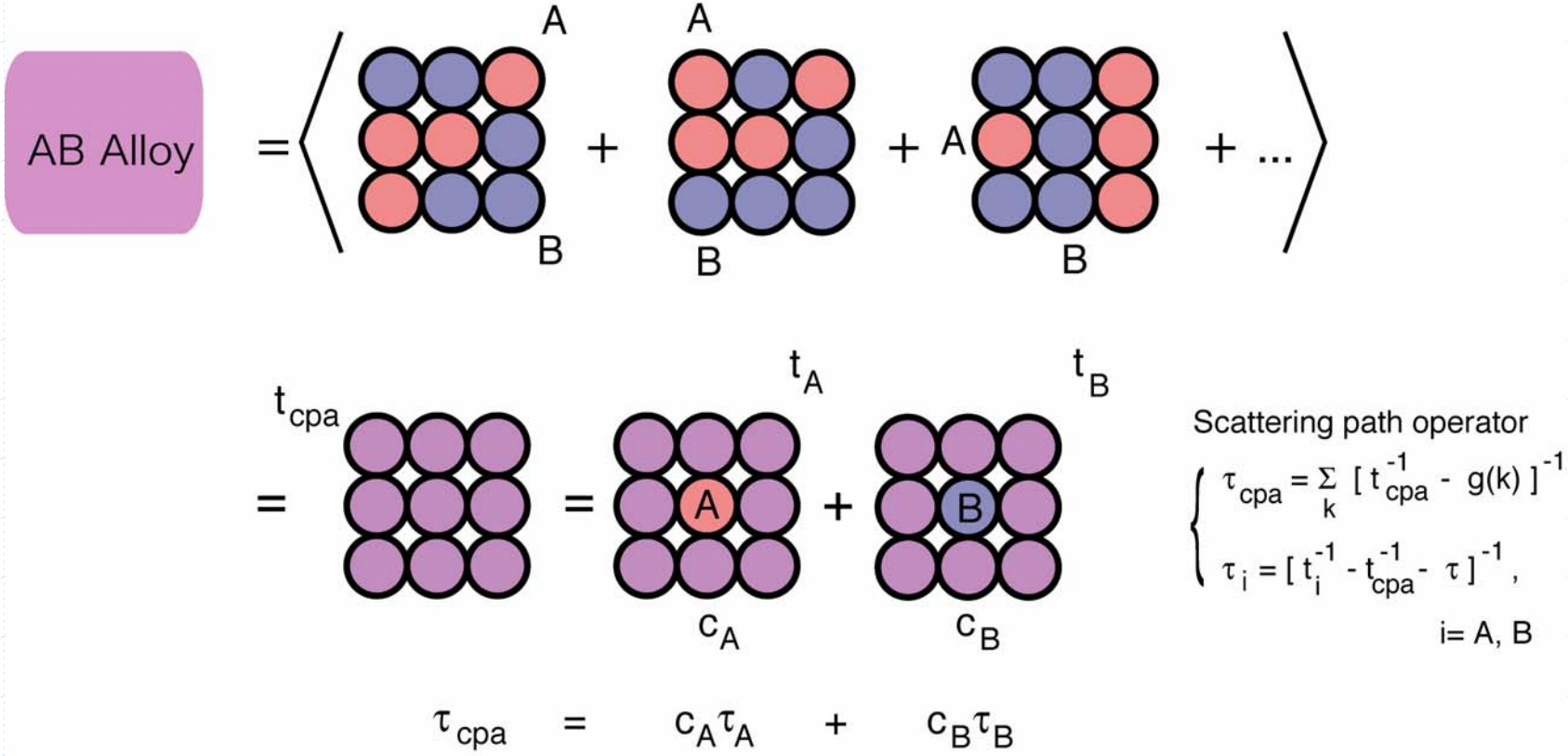

- Electronic structure of substitutional alloy
- Taking configuration average by using multiple scattering technique

Example: Slater-Pauling curve

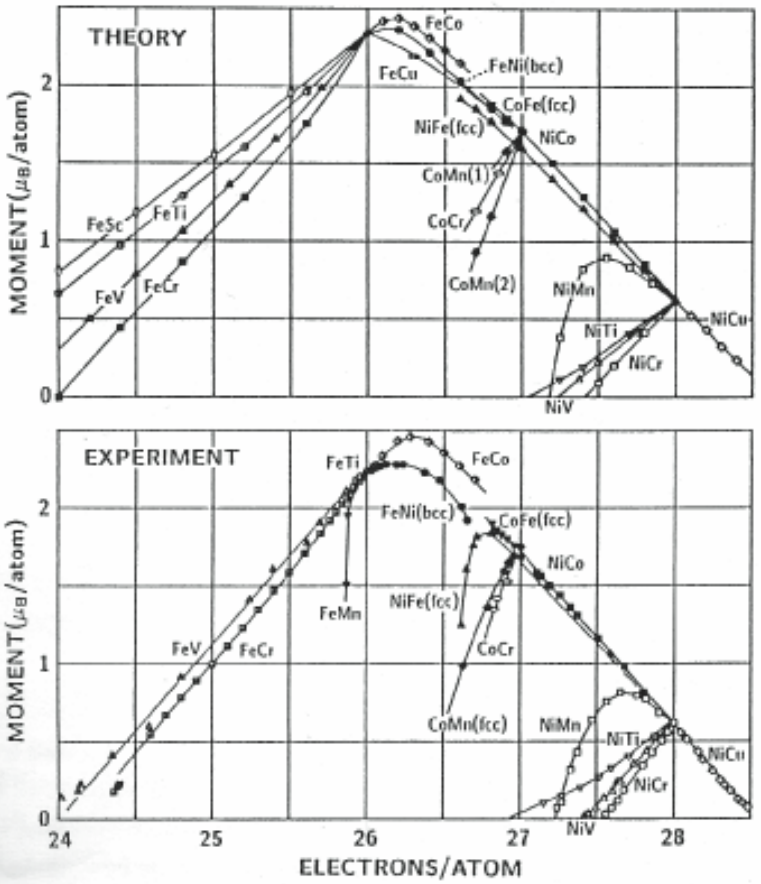

Figure 1. Calculated [10] and experimental saturation magnetization of Fe-, Ni- and Co–based alloys vs. average electron number. The fcc instead of hcp structure is assumed for Co-based alloys. See ref.[10] for further details.

- Magnetic Alloys
- Average magnetic moment behaves regularly
- Theory reproduces experimental curves very well

H. Akai
Hyperfine Interactions 68 (1991) 3.

Disordered local moment state

Paramagnetic state (total magnetization = 0)

H. Akai and P. H. Dederichs: PRB47 (1993) 8739.

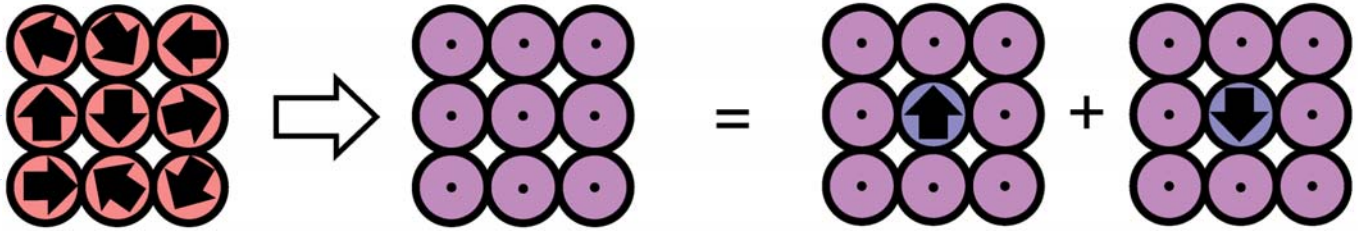

CPA effective medium

Scattering path operator

$$\tau_{cpa} = \frac{1}{2}\tau^{\uparrow} + \frac{1}{2}\tau^{\downarrow}$$

$$\begin{cases} \tau_{cpa} = \sum_k [\, t_{cpa}^{-1} - g(k) \,]^{-1} \\ \tau^i = [\, t_i^{-1} - t_{cpa}^{-1} - \tau_{cpa}^{-1} \,] \quad , \; i = \uparrow \text{ or } \downarrow \end{cases}$$

- Electronic structure above T_C
  - Fe: DLM solution exists ⇒ local moment picture ($\mu = 1.9\mu_B$)
  - Ni: No DLM solution ⇒ Stoner picture ($\mu = 0$)
- Energy difference between FM and DLM states ⇒ T_C

Mapping on Heisenberg model

$$H = -\sum_{i \neq j} J_{ij} \boldsymbol{e}_i \cdot \boldsymbol{e}_j$$

J_{ij}: exchange interaction
e_i: direction of the moment

- How to calculate J_{ij}
  - Finite rotation (Oguchi et al.)
  - Infinitesimal rotation (Liechtenstein et al.)
  - Frozen magnon approach (Sandratskii et al.)
- Curie temperature
  - Mean field approximation

$$k_B T_C = \frac{2c}{3} \sum_{i \neq 0} J_{0i}$$

  - Random phase approximation

$$k_B T_C = \frac{2c}{3} \left(\frac{1}{N} \sum_{\boldsymbol{q}} [J(\boldsymbol{0}) - J(\boldsymbol{q})]^{-1} \right)^{-1}$$

$$J(\boldsymbol{q}) \equiv \sum_{i \neq 0} J_{0i} \exp(i\boldsymbol{q} \cdot \boldsymbol{R}_{0i})$$

  - Monte Carlo simulation(exact)

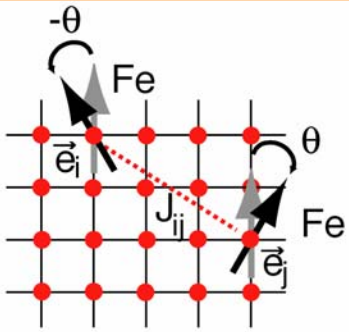

t: single site t-matrix
τ: scattering path operator
g: KKR structure constant
$\vec{R}$: lattice vector

$$J_{ij} = \frac{1}{4\pi} \mathrm{Im} \int^{\varepsilon_F} d\varepsilon \, \mathrm{Tr} \left[\Delta_i(\varepsilon) \tau_{ij}^{\uparrow}(\varepsilon) \Delta_j(\varepsilon) \tau_{ji}^{\downarrow}(\varepsilon) \right]$$

$$\begin{cases} \Delta_i(\varepsilon) = t_{i\uparrow}^{-1}(\varepsilon) - t_{i\downarrow}^{-1}(\varepsilon) \\ \tau_{ij}(\varepsilon) = \sum_{\vec{k}} \left[t^{-1}(\varepsilon) - g(\vec{k}, \varepsilon) \right]^{-1} \exp\{ i \vec{k} \cdot (\vec{R}_i - \vec{R}_j) \} \end{cases}$$

Liechtenstein et al., JMMM 67 (1987) 65

Example: Typical ferromagnetic metals

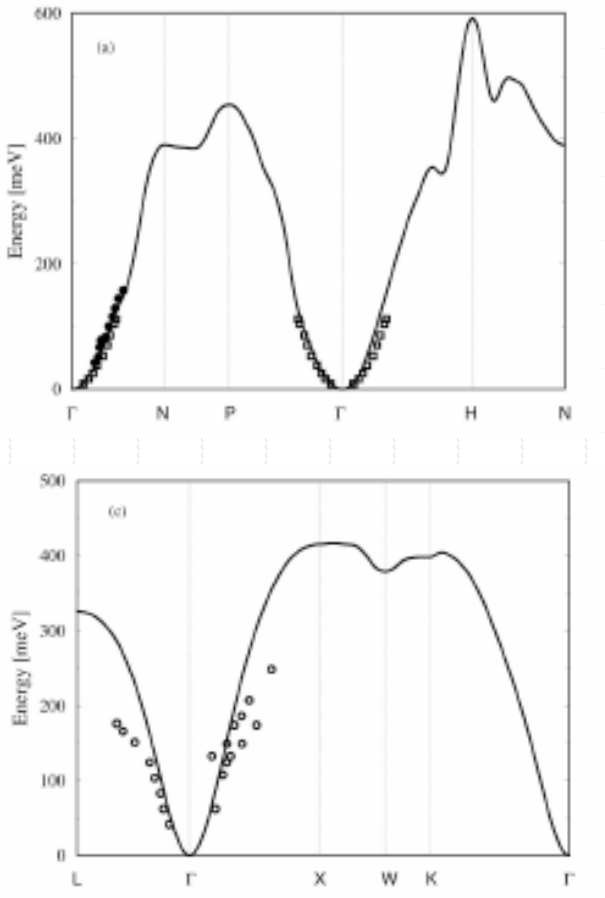

FIG. 1. Magnon-dispersion relations along high-symmetry lines in the Brillouin zone: (a) bcc Fe (experiment: Ref. 33, 10 K, filled circles and Ref. 35, Fe(12% Si), room temperature, empty squares); (b) fcc Co; and (c) fcc Ni (experiment: Ref. 34, room temperature, empty circles). Lines are calculated results.

- Fe, Co, Ni
  - Exchange interactions
  - Curie temperature
  - Magnon-dispersion relation

TABLE II. Calculated spin-wave stiffness constants (D_{th}) and Curie temperatures (T_C^{MFA} and T_C^{RPA}) and their comparison with experimental values D_{ex} and T_C^{ex}.

Metal	D_{th} (meV Å^2)	D_{ex} (meV Å^2)	T_C^{MFA} (K)	T_C^{RPA} (K)	T_C^{ex} (K)
Fe (bcc)	250±7	280,[a] 330[b]	1414	950±2	1044–1045
Co (fcc)	663±6	580,[c,a] 510[b]	1645	1311±4	1388–1398[c]
Ni (fcc)	756±29	555,[d] 422[a]	397	350±2	624–631

[a]Magnetization measurement (Ref. 37) at 4.2 K.
[b]Neutron-scattering measurement extrapolated to 0 K (Ref. 38).
[c]Data refer to hcp Co at 4.2 K.
[d]Neutron-scattering measurement at 4.2 K (Ref. 36).

Pajda et al., Phys. Rev. B64 (2001) 174402

Dilute magnetic semiconductors

- Dilute magnetic semiconductors → Spintronics
- (Ga, Mn)As, (In, Mn)As: T_C < room temp.

Dietl et al., Zener p-d model in MFA, Science 287 (2000) 1019.

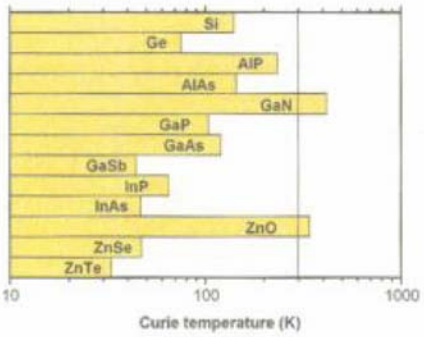

Fig. 3. Computed values of the Curie temperature T_C for various p-type semiconductors containing 5% of Mn and 3.5×10^{20} holes per cm^3.

K. Sato et al., KKR-CPA-LDA JJAP 40 (2001) L485.

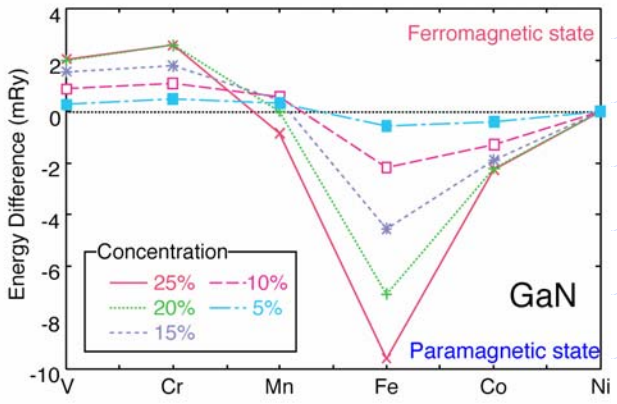

Ab initio technique for finite temperature magnetism

- ✓ Origin of ferromagnetism in DMS
- ✓ Accurate T_C calculations for DMS
- ✓ Effect of inhomogeneous impurity distribution in DMS

Electronic structure calculation

- Local spin density approximation (LSDA)
- Korringa-Kohn-Rostoker method (KKR)
- Coherent-potential-approximation (CPA)
  - ➔ MACHIKANEYAMA2002 by Akai

(Ga, Mn)As DMS

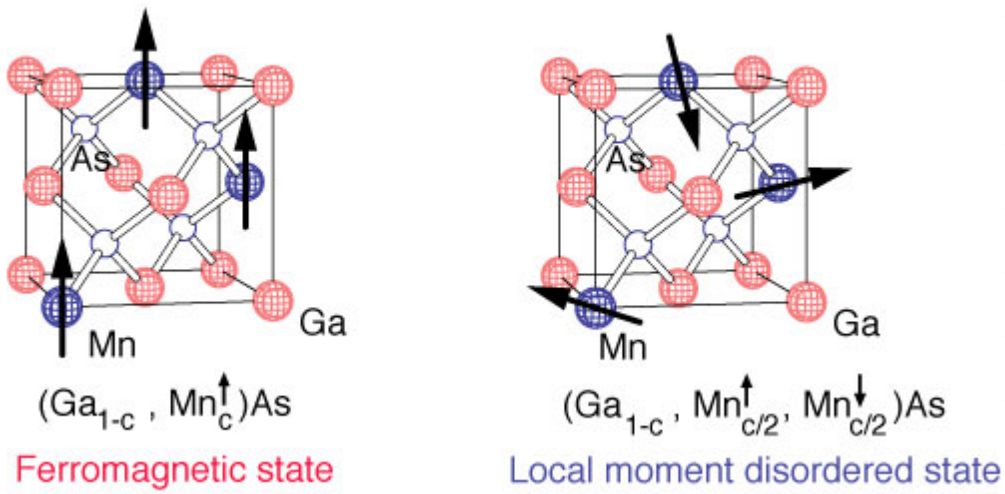

Stability of ferromagnetic state: ΔE = TE(DLM) - TE(FM)

Coherent potential approximation

- Dilute magnetic semiconductors
  - Substitutional disorder + Magnetic disorder (paramagnetic state)

Ferromagnetic DMS (total magnetization ≠ 0)

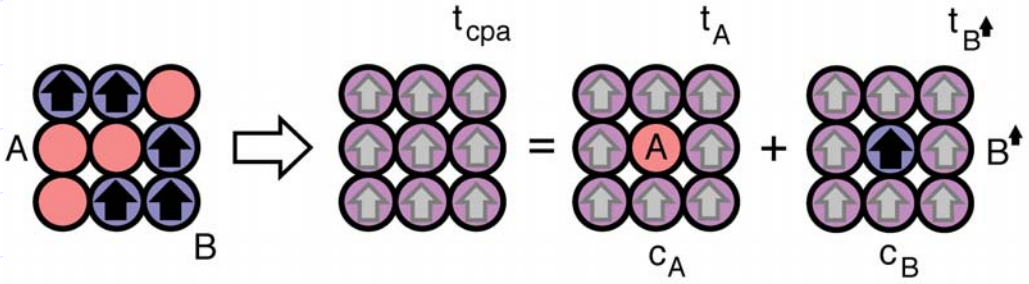

$$\tau_{cpa} = c_A\tau_A + c_B\tau_{B\uparrow}$$

Scattering path operator

$$\begin{cases} \tau_{cpa} = \sum_k [\, t_{cpa}^{-1} - g(k)\,]^{-1} \\ \tau = [\, t_i^{-1} - t_{cpa}^{-1} - \tau\,]^{-1}, \end{cases}$$

i= A, B

Paramagnetic DMS (total magnetization = 0)

H. Akai and P. H. Dederichs: PRB47 (1993) 8739.

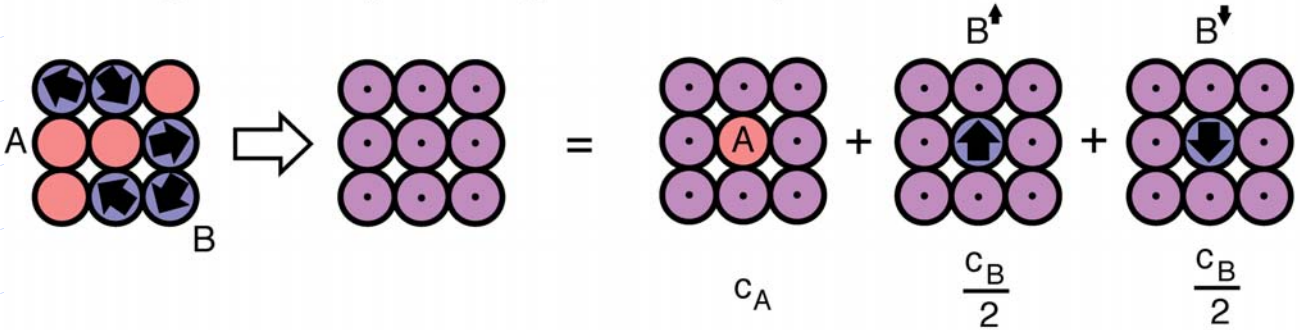

$$\tau_{cpa} = c_A\tau_A + \frac{c_B}{2}\tau_{B\uparrow} + \frac{c_B}{2}\tau_{B\downarrow}$$

T_C in mean field approximation

Classical Heisenberg model

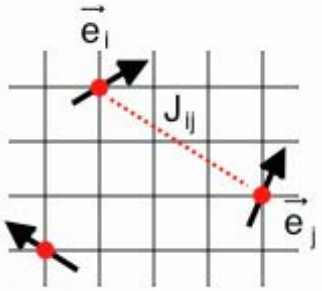

$$H = -\sum_{i \neq j} J_{ij}\, \vec{e}_i \cdot \vec{e}_j$$

J_{ij} : exchange interaction

$\vec{e}_i$: direction of local magnetic moment at site i

Mean Field Approximation (MFA)

A. Total energy difference

$$\langle H \rangle_{FM} = -\sum_{i \neq j} J_{ij} \langle \vec{e}_i \rangle \cdot \langle \vec{e}_j \rangle = -c^2 N \sum_{i \neq 0} J_{i0} \qquad \langle H \rangle_{LMD} = 0$$

c : concentration of magnetic ions
N : Number of lattice sites

$$\Delta E = [\, -\langle H \rangle_{FM} + \langle H \rangle_{LMD} \,] / N = c^2 \sum_{i \neq 0} J_{i0}$$

B. Curie temperature (Molecular field theory)

$$k_B T_C^{MFA} = \frac{2}{3} c \sum_{i \neq 0} J_{i0} = \frac{2}{3} \frac{\Delta E}{c}$$

T_C^{MFA} of Mn-doped III-V DMS

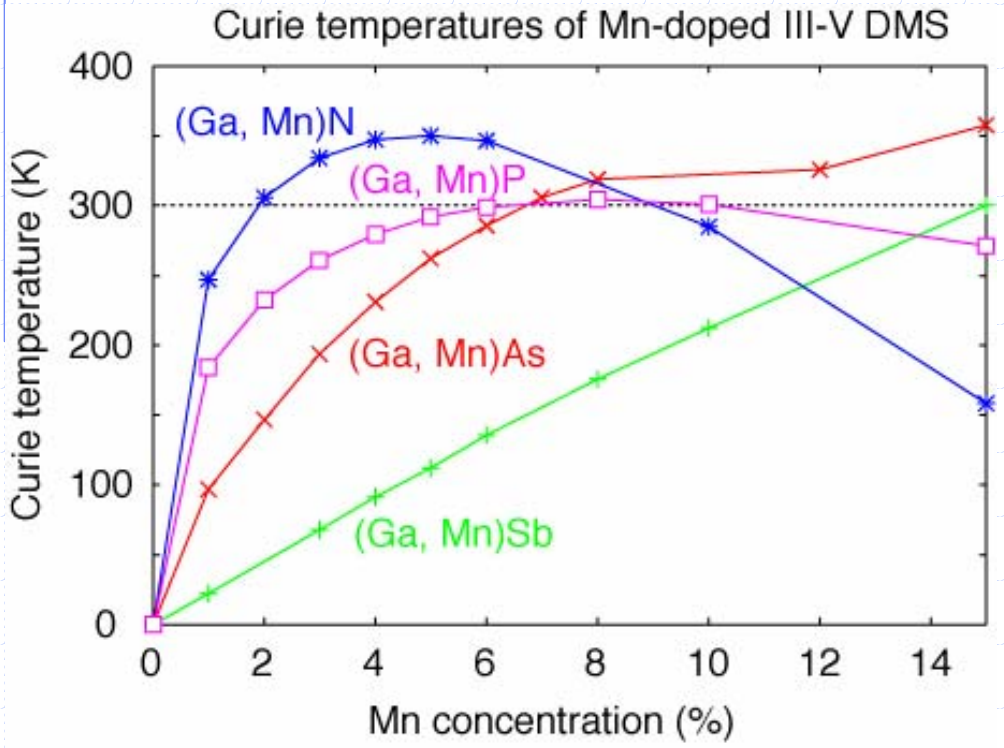

(Ga, Mn)N; Tc ~ √c

(Ga, Mn)Sb; Tc ~ c

↕

Electronic structure

- Origin of the ferromagnetism
  - double exchange
  - p-d exchange

Electronic structure of DMS

Impurity band
in the gap → double exchange

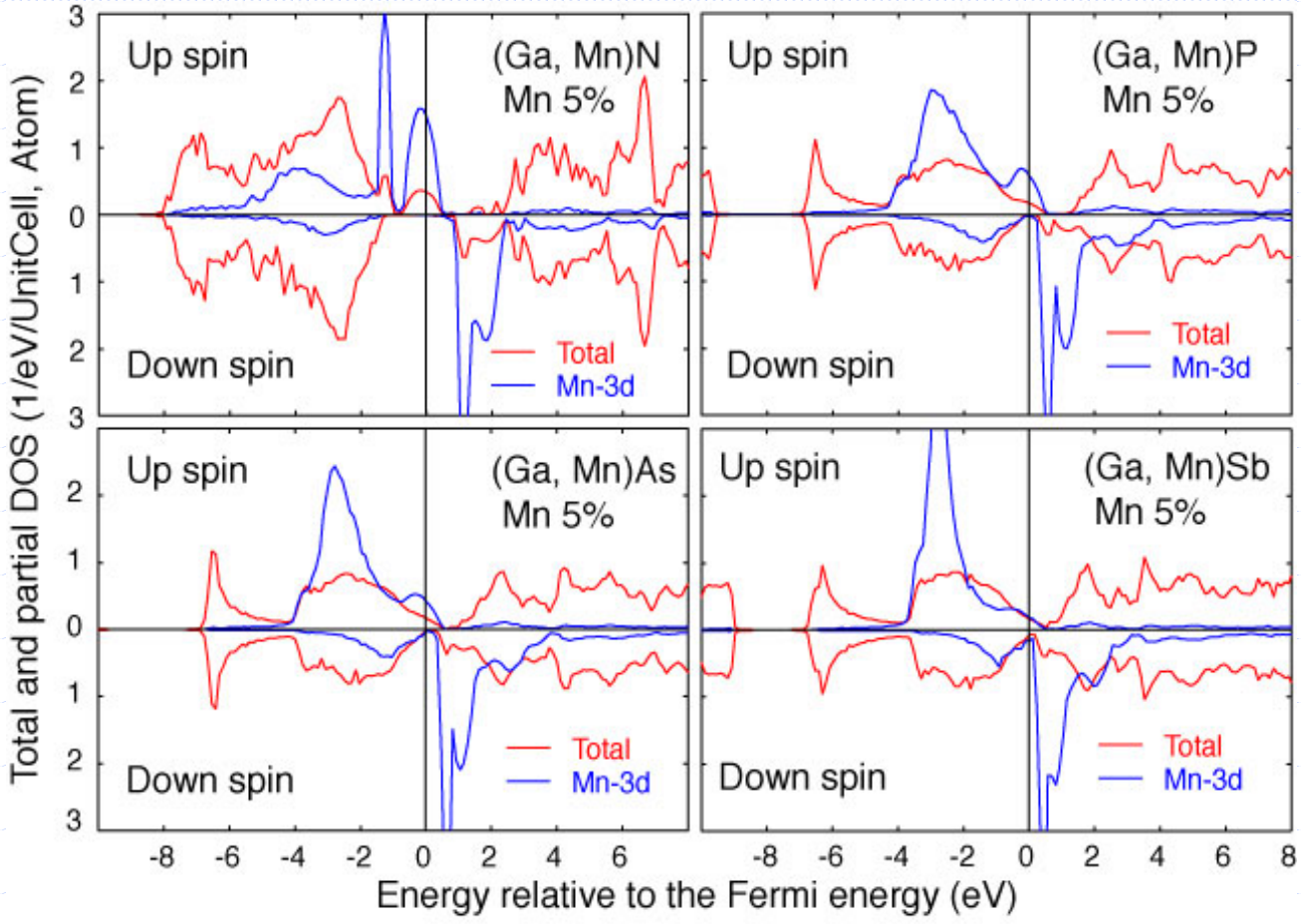

Localized d-states
below valence band → p-d exchange

Ferromagnetism in DMS

Mechanism

Double exchange mechanism [1,2]

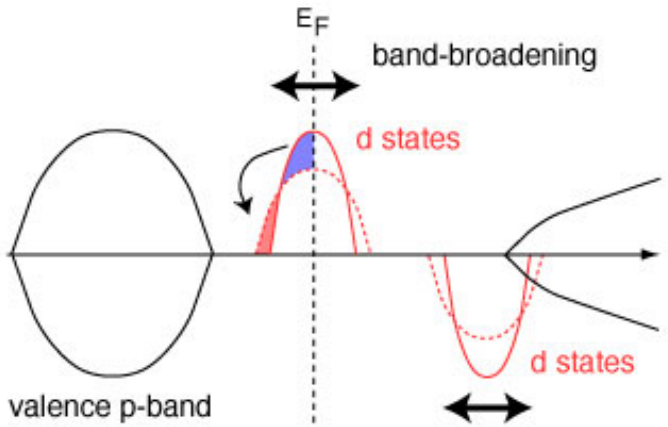

Band energy change in impurity d-band

Band energy gain ~ W ~ $c^{1/2}$

(if E_F is in impurity band)

p-d exchange mechanism [3,4]

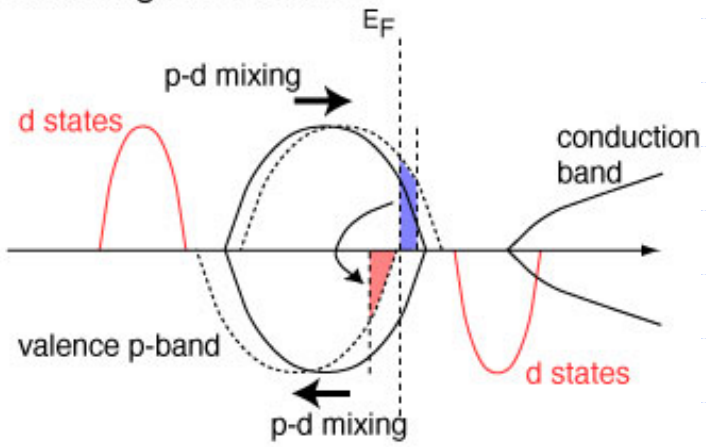

Hole mediated ferromagnetism

Band energy change in valence band

Half-metallic system

Valence band is polarized : -1 μ_B / Mn

Average polarization (mean field) : -c μ_B

Interaction between Mn ions ~ c

1. H. Akai, PRL 81 (1998) 3002. 2. K. Sato and H. K.-Yoshida, Jpn. J. Appl. Phys. 40 (2001) 485.
3. T. Dietl et al., Science 287 (2000) 1019. 4. J. Kanamori and K. Terakura, J. Phys. Soc. Jpn. 70 (2001) 1433.

Calculation for exchange interactions

- Magnetic force theorem
- Mapping on effective Heisenberg model

A. I. Liechtenstein et al. JMMM 67(1987)65.

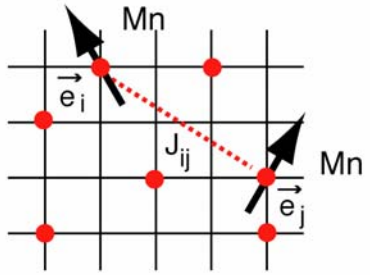

Mn random distribution

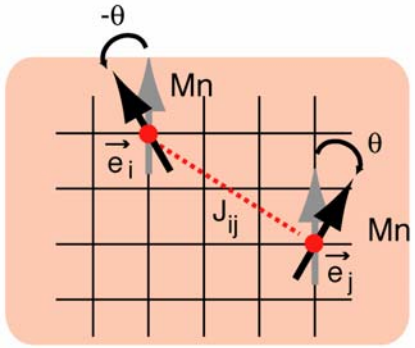

CPA medium

$$J_{ij} = \frac{1}{4\pi} \mathrm{Im} \int^{\varepsilon_F} d\varepsilon \, \mathrm{Tr} \left[\Delta_i(\varepsilon) \tau^{\uparrow}_{ij}(\varepsilon) \, \Delta_j(\varepsilon) \, \tau^{\downarrow}_{ji}(\varepsilon) \right]$$

$$\begin{cases} \Delta_i(\varepsilon) = t^{-1}_{i\uparrow}(\varepsilon) - t^{-1}_{i\downarrow}(\varepsilon) \\ \tau_{ij}(\varepsilon) = \left[t^{-1}(\varepsilon) - \tilde{t}^{-1}(\varepsilon) + \tilde{\tau}^{-1}(\varepsilon) \right]^{-1}_{ij} \\ \tilde{\tau}_{ij}(\varepsilon) = \sum_{\vec{k}} \left[\tilde{t}^{-1}(\varepsilon) - g(\vec{k}, \varepsilon) \right]^{-1} \exp\{ i \vec{k} \bullet (\vec{R}_i - \vec{R}_j) \} \end{cases}$$

t: single site t-matrix
τ: scattering path operator
$\tilde{t}$: cpa single site t-matrix
$\tilde{\tau}$: cpa scattering path operator
$\vec{R}$: lattice vector
g: KKR structure constant

Exchange interactions in DMS

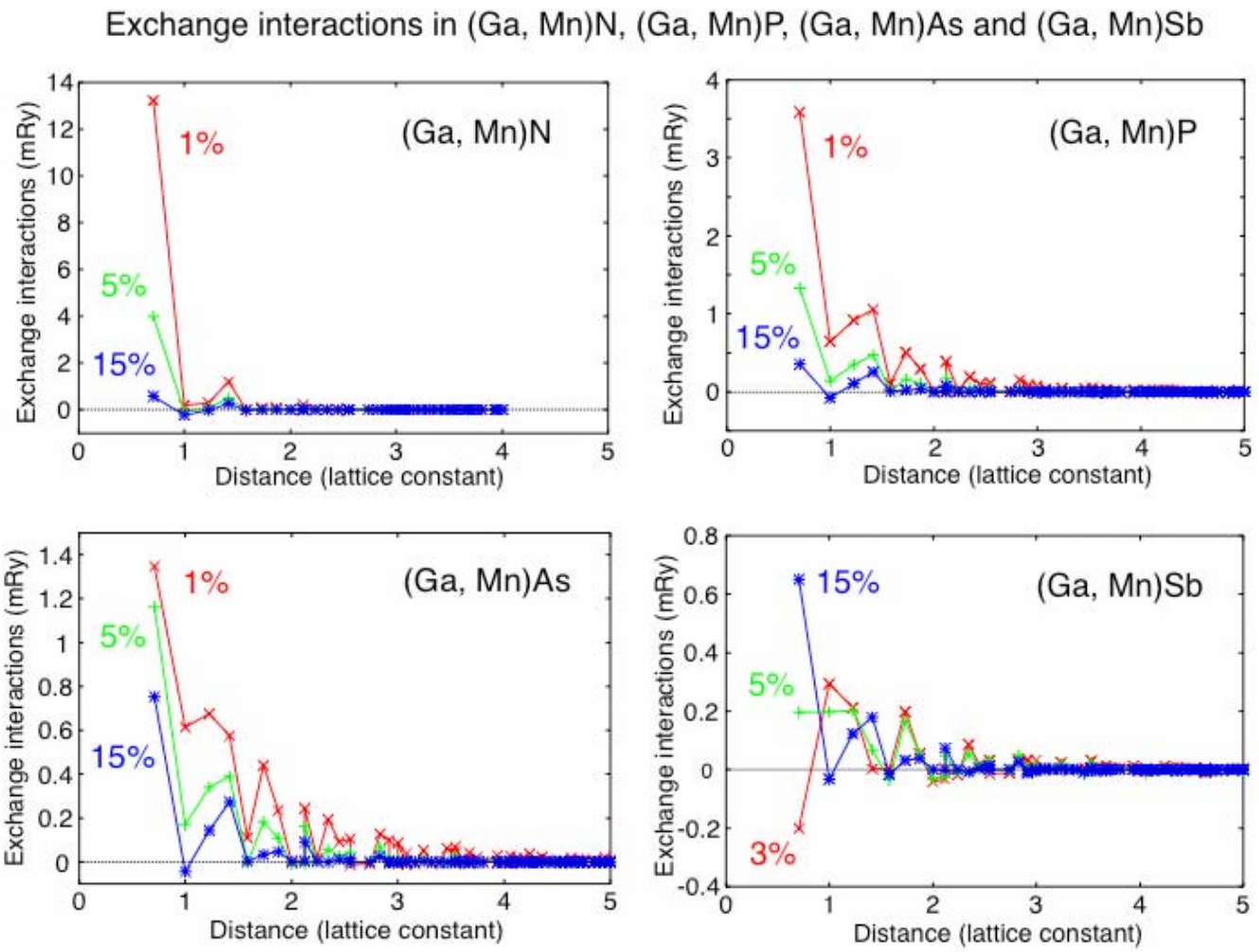

- Double exchange system (Ga, Mn)N → strong, but short-ranged interactions
- p-d exchange system (Ga, Mn)Sb → weak, but long-ranged interactions

Magnetic percolation problem

- 2D square lattice with nearest neighbor interaction.

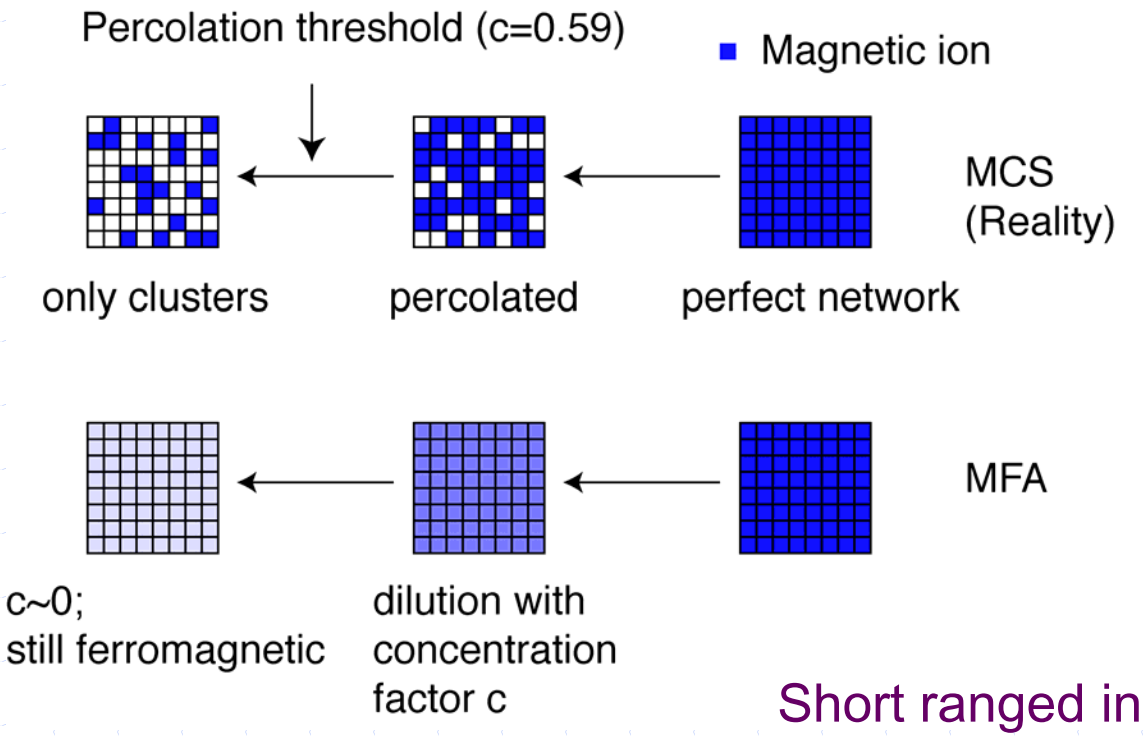

lattice	percolation threshold
square	0.59
triangle	0.50
diamond	0.43
sc	0.31
bcc	0.25
fcc	0.20

Short ranged interaction
→ Ferromagnetism is suppressed
below the percolation threshold

Nearest neighbor Heisenberg model

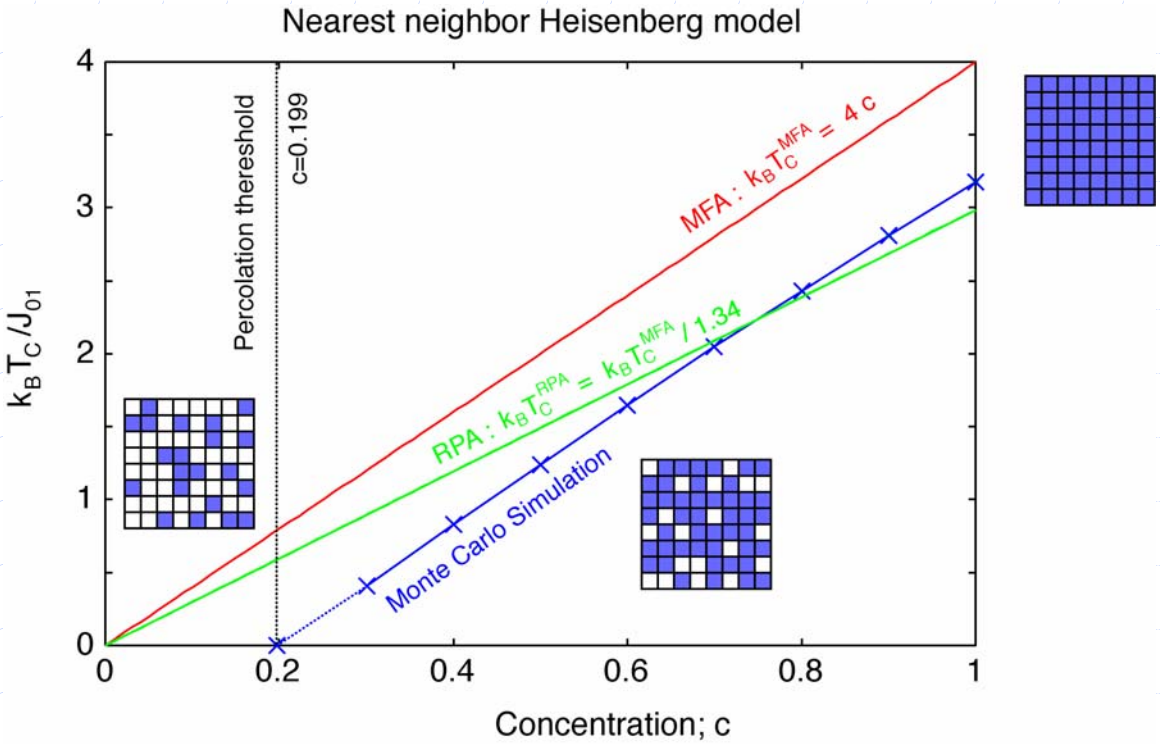

- c~1, MFA values are reasonable
- Ferromagnetism disappears below the percolation threshold

Monte Carlo simulation

Thermal average of physical observable A

$$\langle A \rangle = \frac{1}{Z}\int dx \exp\left[-H(x)/k_B T\right] A(x) = \frac{\sum_{i=1}^{M} \exp\left[-H(x_i)/k_B T\right] A(x_i)}{\sum_{i=1}^{M} \exp\left[-H(x_i)/k_B T\right]}$$

Z: partition function k_B : Boltzmann constant
H: model Hamiltonian T: temperature

Metropolis algorithm ..... efficient sampling technique in the phase space

1) Prepare a simulation box.

$$H = -\sum_{i \neq j} J_{ij}\, \vec{e}_i \cdot \vec{e}_j$$

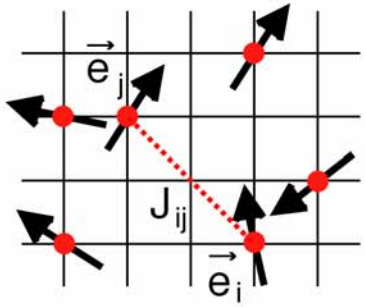

2) Choose a site i, and calculate the energy change ΔE due to a random rotation of the magnetic moment.

3) Generate random number r between 0 and 1.

4) If $r < \exp[-\Delta E/k_B T]$, rotate the moment.

5) Analyze the resulting configuration and store the property for the averaging.

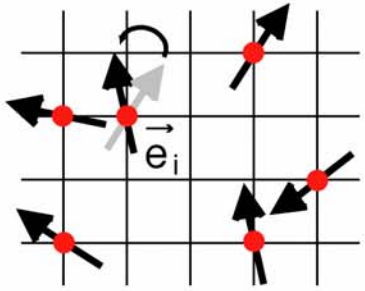

Exact T_C values taking disorder effect fully into account

T_C by Monte Carlo Simulation

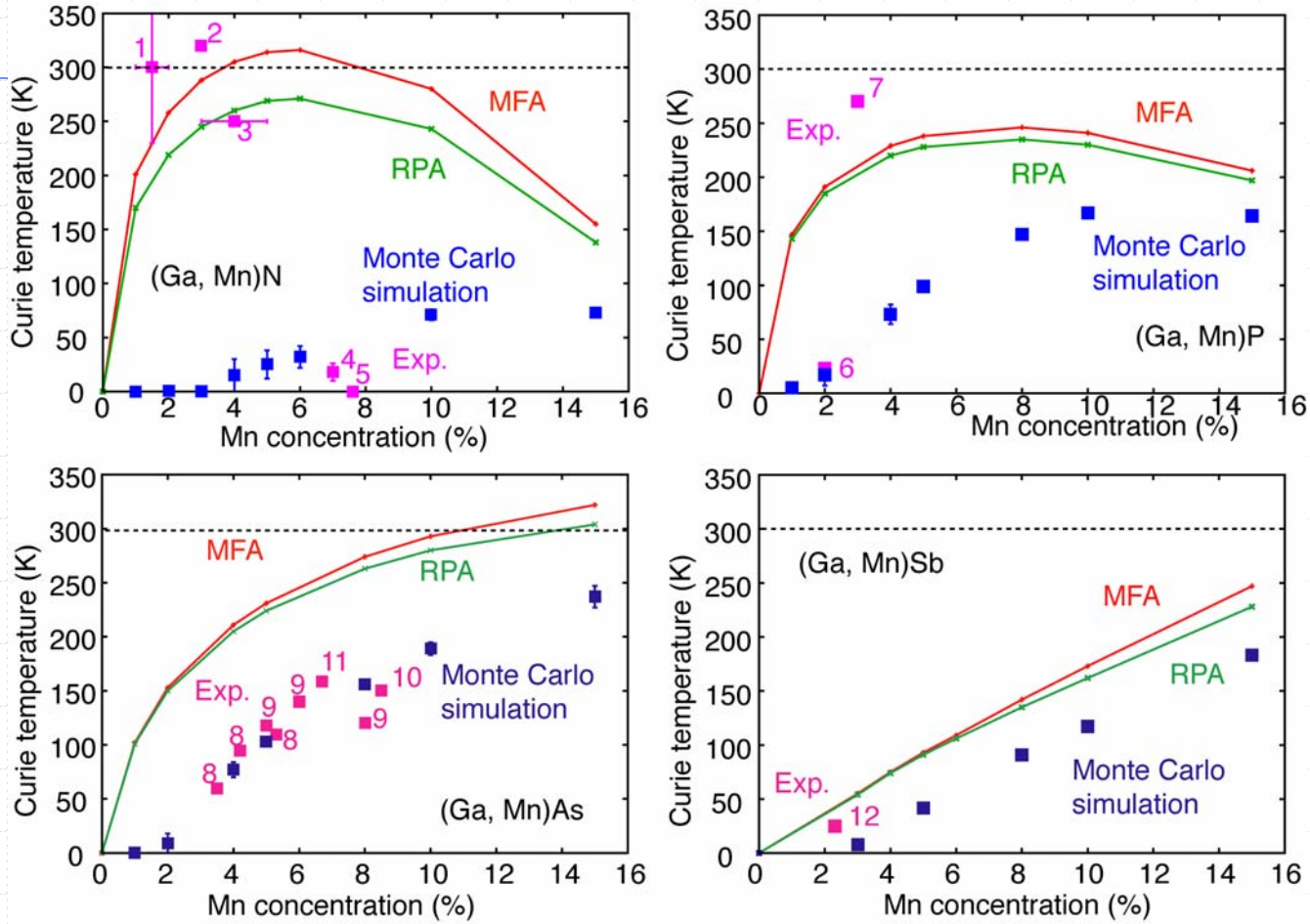

Experimental values:
1. Reed et al. APL 79 (2001) 3473. 2. Thaler et al. APL 80 (2002) 3964. 3. Theodoropoulou et al. APL (2001) 3475. 4. Overberg et al. APL 79 (2001) 1312.
5. Ploog et al. J. Vac. Sci. Technol. B21 (2003) 1756. 6. Scarpulla et al. Physica B340 (2003) 908. 7. Theodoropoulou et al. PRL 89 (2002) 107203. 8. Matsukura et al. PRB 57 (1998) R2037.
9. Edmonds et al. APL 81 (2002) 4991. 10. Ku et al. APL 82 (2993) 2302. 11. Edmonds et al. PRL 92 (2004) 37201. 12. Abe et al. Physica E7 (2000) 981.

Reasonable agreement with experiments.

High-T_C phases can not be explained.

Inhomogeneous impurity distribution in DMS

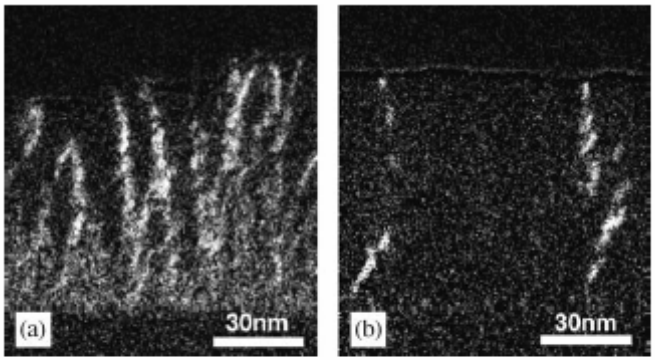

Fig. 1. Energy-filtered electron micrographs showing Cr segregation in Al(Cr)N films grown at 700 °C: (a) 7% Cr-doped AlN; (b) 2.5% Cr-doped AlN.

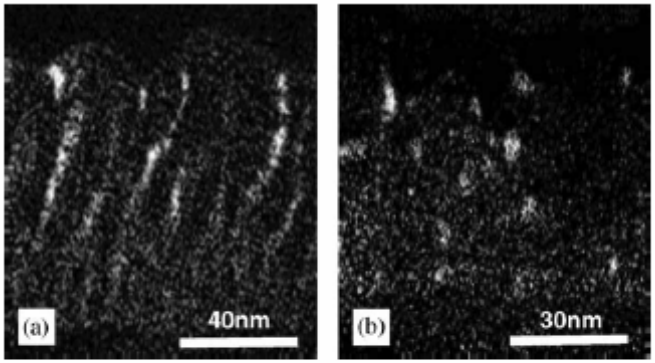

Fig. 2. Energy-filtered electron micrographs showing Cr distribution for 4% Cr-doped AlN grown at different substrate temperatures: (a) 700 °C; (b) 800 °C.

Gu et al., JMMM 290-291(2005)1395.

- MBE
- (Al, Cr)N, Cr 7%, Tc>900K
- (Ga, Cr)N, Cr 3%, Tc>900K
- TEM, EELS
- One-dimensional Cr-rich region: Ferromagnetic
- Spherical clusters:not FM

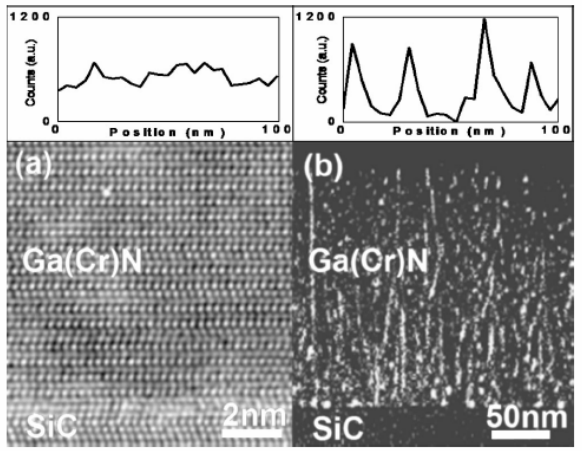

FIG. 3. (a) HRTEM image and (b) energy-filtered TEM image showing Cr distribution in GaN film grown at 775 and 825 °C, respectively. EELS line profile analysis of Cr is shown as inset.

Singh et al., APL 86 (2005)12504

Generalized perturbation method

Ducastelle and Gautier: 'Generalized perturbation method'
J. Phys. F6 (1976) 2039

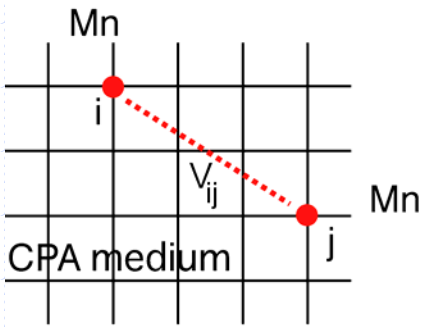

$$H = - \sum_{i \neq j} V_{ij} \, \sigma_i \, \sigma_j$$

$$V_{ij} = V_{ij}^{AA} + V_{ij}^{BB} - 2V_{ij}^{AB}$$

V_{ij} : Effective pair interaction between site i and j

σ_i : Occupation number

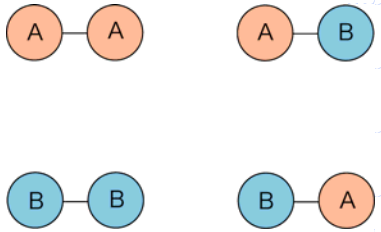

$$V_{ij} = \frac{-2}{\pi} \, \mathrm{Im} \int^{\varepsilon_F} d\varepsilon \, \mathrm{Tr} \left[\Delta_i(\varepsilon) \tau_{ij}(\varepsilon) \, \Delta_j(\varepsilon) \, \tau_{ji}(\varepsilon) \right]$$

$$\begin{cases} \Delta_i(\varepsilon) = X_A^i(\varepsilon) - X_B^i(\varepsilon) \\ \tau_{ij}(\varepsilon) = \sum_{\vec{k}} \left[t^{-1}(\varepsilon) - g(\vec{k}, \varepsilon) \right]^{-1} \exp\{ i \vec{k} \bullet (\vec{R}_i - \vec{R}_j) \} \end{cases}$$

X: single site scattering-matrix $\vec{R}$: lattice vector
τ: scattering path operator g: KKR structure constant

Turchi et al., PRL 67 (1991) 1779.

Effective pair interaction in DMS

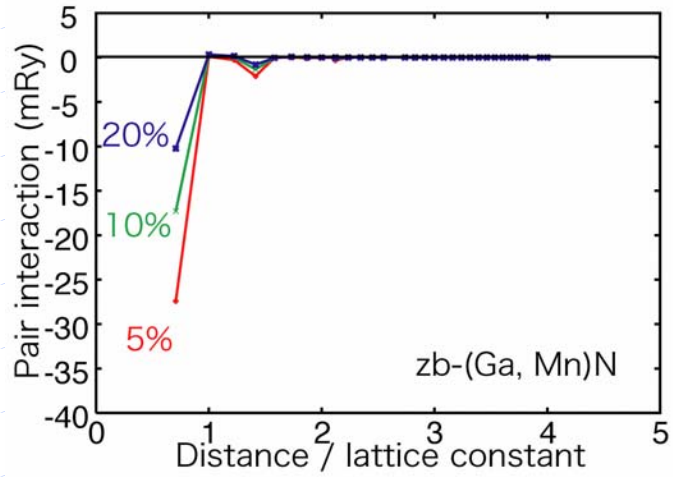

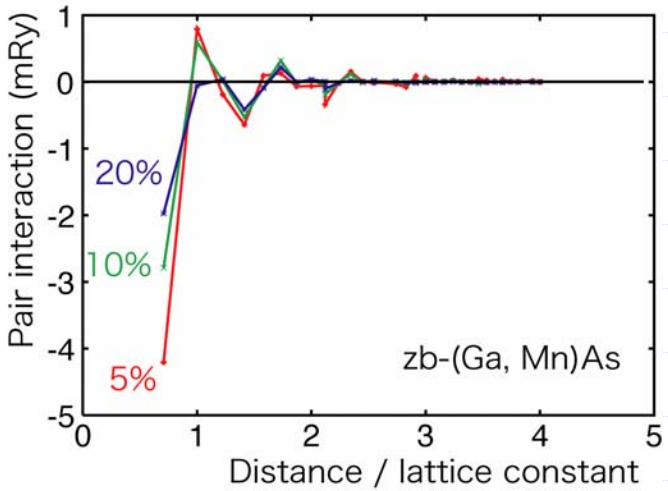

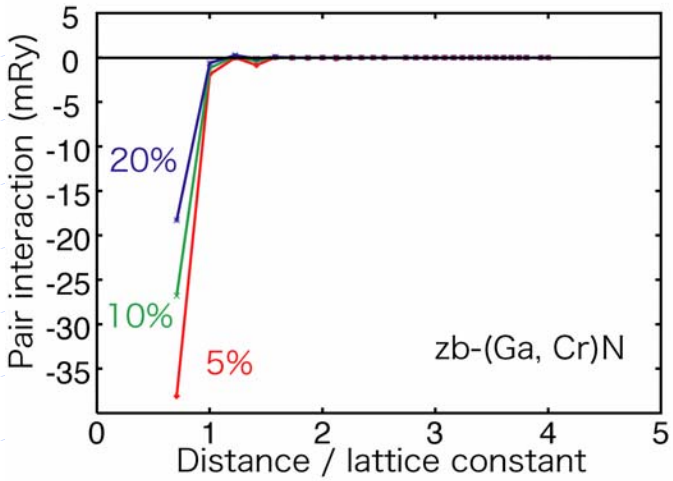

Effective attractive interactions between nearest neighbors
→tendency toward phase separation

M. van Schilfgaarde et al., PRB 63 (2001) 233205.

H. Raebiger et al., JMMM 290-291 (2005) 1398.

Generate inhomogeneous distribution

SImulation of spinodal decomposition

1) Prepare a simulation box.

$$H = - \sum_{i \neq j} V_{ij} \, \vec{\sigma}_i \cdot \vec{\sigma}_j$$

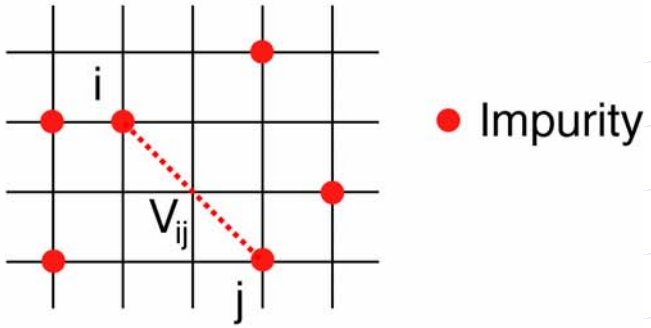

2) Choose a site i, and try to move it to one of the nearest neighbor sites.
Calculate the energy change ΔE due to the transfar.

3) Generate random number r between 0 and 1.

4) If $r < \exp[-\Delta E/k_B T]$, rotate the moment.

5) Store the resulting configuration and calculate magnetic properties.

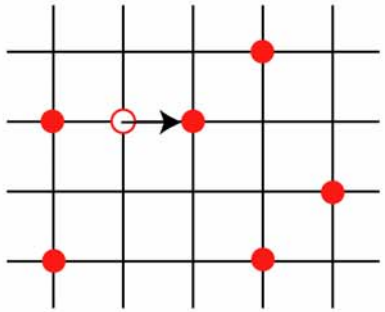

Spinodal decomposition in (Ga, Mn)N

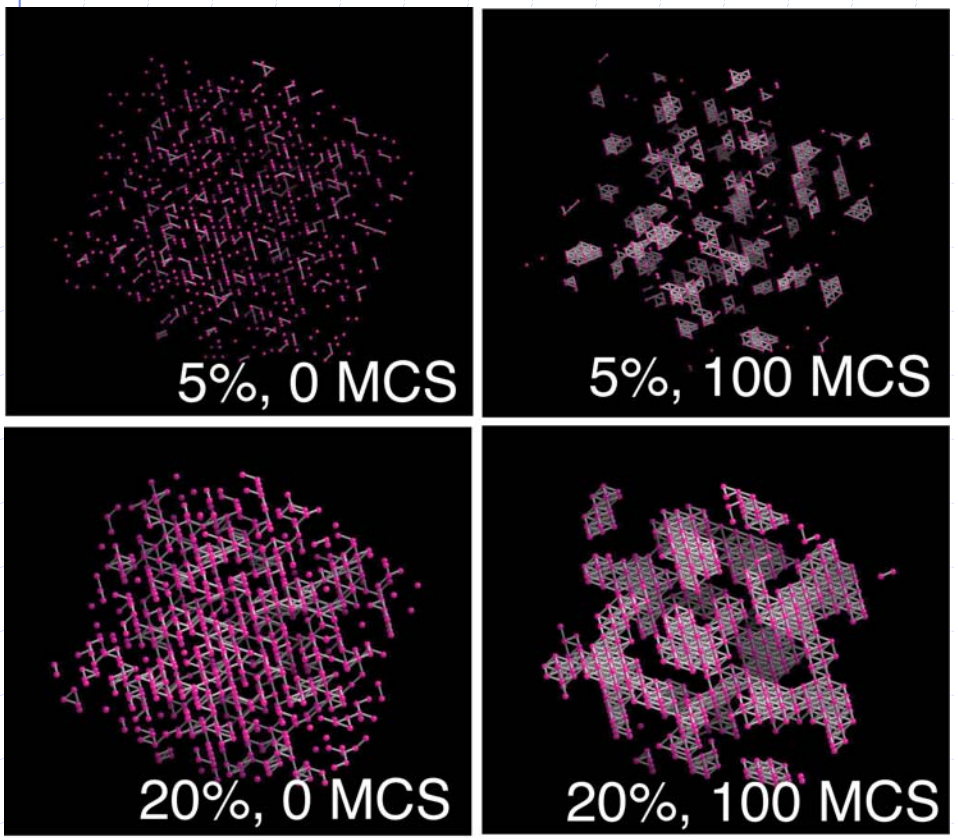

- Low concentration (5%)
  - Small clusters
  - No percolation
  - No T_C enhancement is expected.
- High concentration (20%)
  - Connecting random pattern
  - Magnetic network
  - T_C enhancement

annealing of bulk sample

Effects of spinodal decomposition on T_C

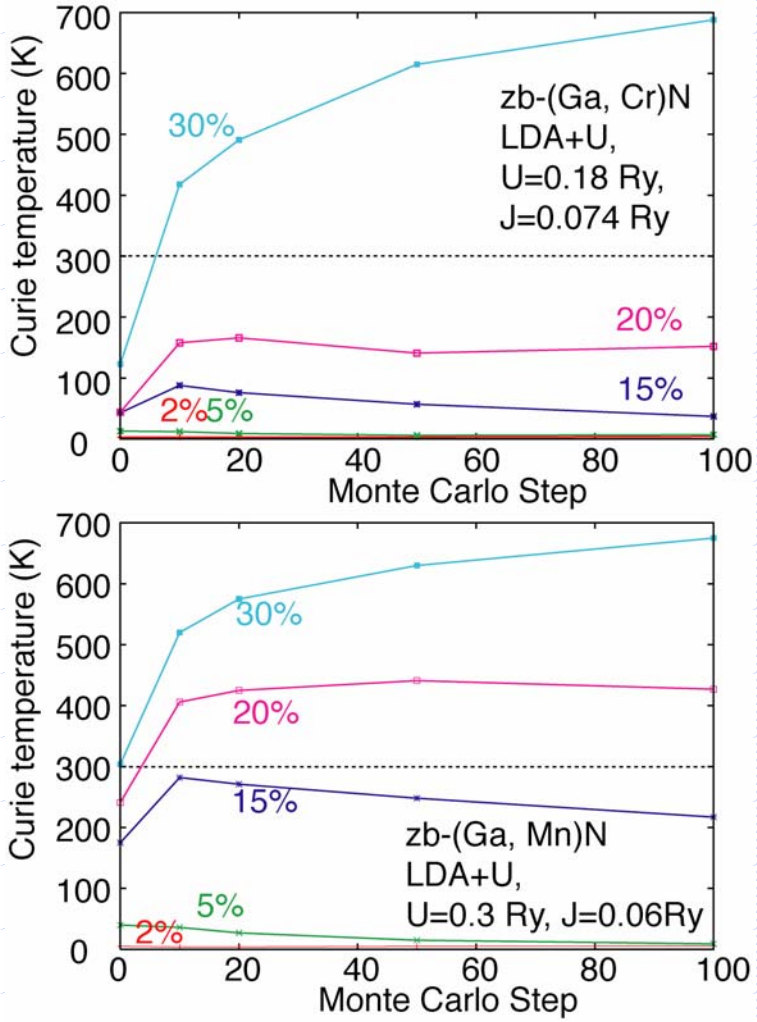

- Low concentration (5%)
  - Small clusters
  - No percolation
  - No T_C enhancement is expected.
- High concentration (20%)
  - Connecting random pattern
  - Magnetic network
  - T_C enhancement

Layer by layer growth condition

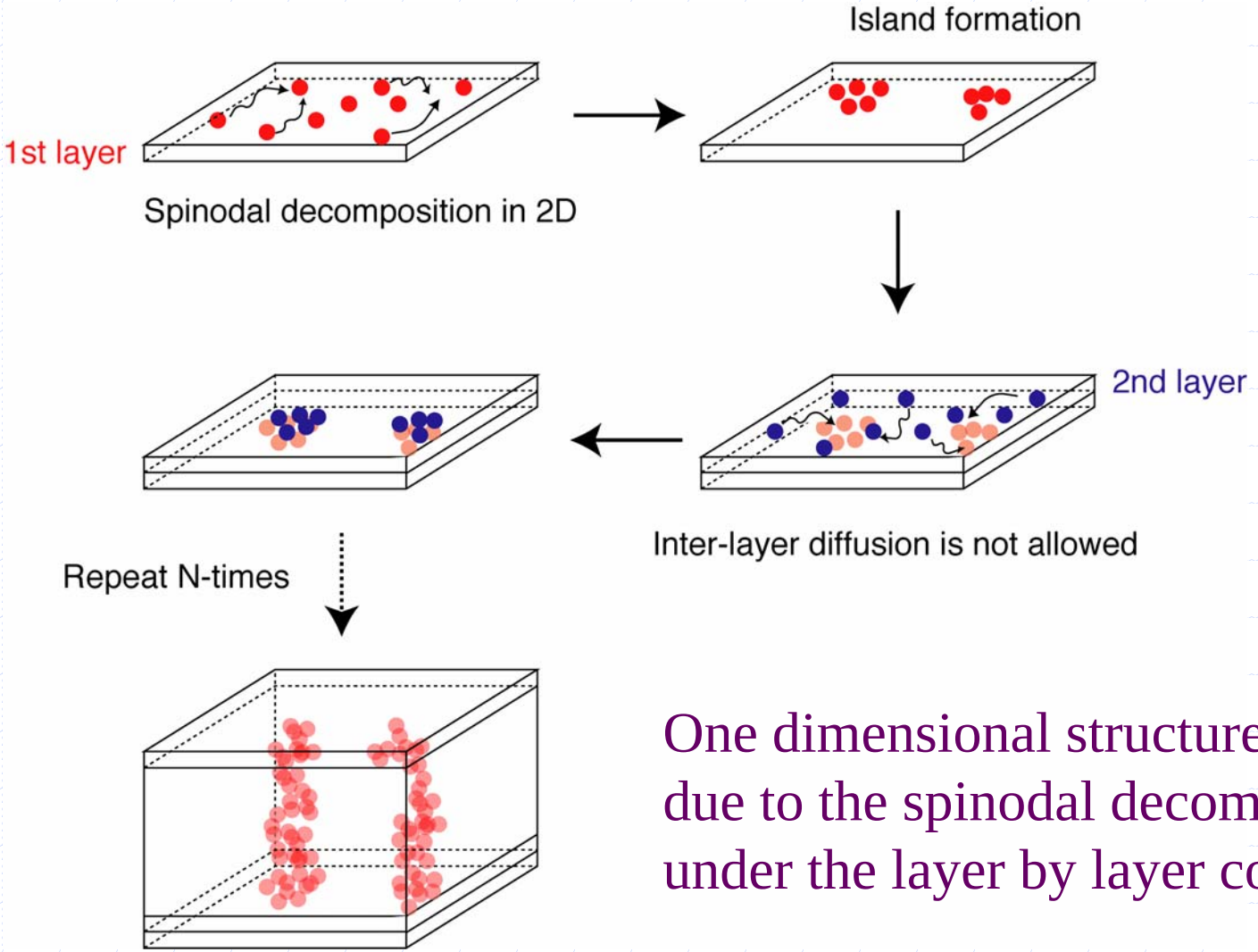

One dimensional structure
due to the spinodal decomposition
under the layer by layer condition.

Layer by layer growth simulation

(Zn, Cr)Te, Cr 5%

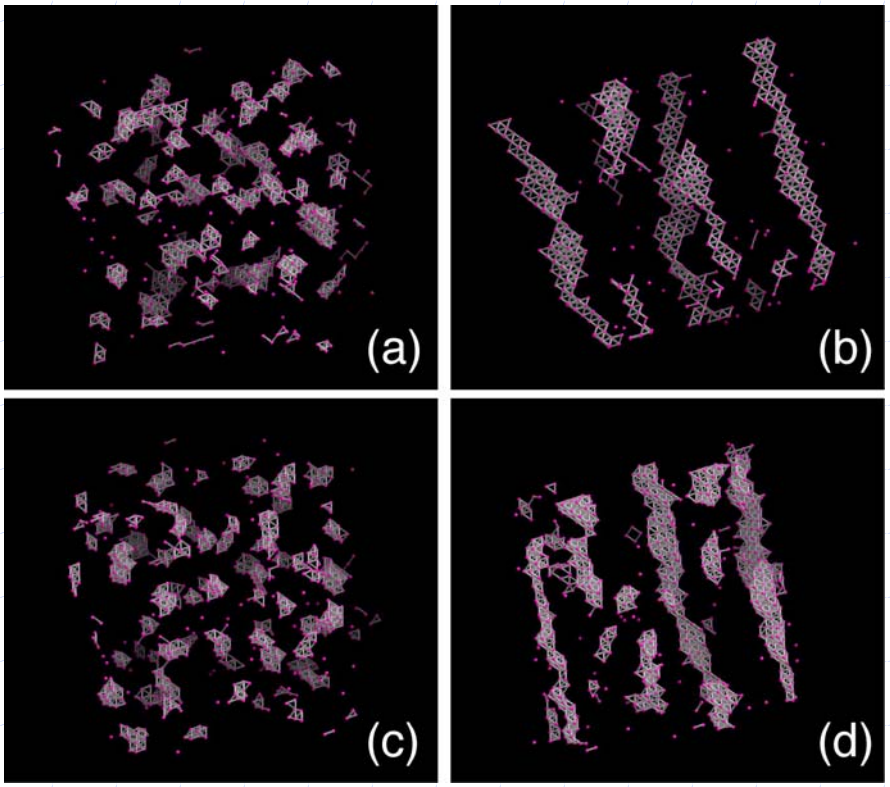

(Ga, Mn)N, Mn 5%

- Spinodal decomposition in 3D
  - Small clusters
  - No percolation
  - No T_C enhancement
- Layer by layer growth simulation
  - One dimensional fragments
  - Magnetic network
  - No T_C enhancement
  - Strong anisotropy

↓

Super paramagnetic blocking phenomena

Summary

- Ab initio simulation of finite temperature magnetism
  - Disordered local moment technique
  - Mapping on Heisenberg model + statistical method
- Application to dilute magnetic semiconductors
  - Mechanism and T_C calculations
  - Impurity band in the gap
    → double exchange → short ranged interaction
  - Localized moment
    → p-d exchange → long ranged interaction
  - Low concentration, Low T_C (Magnetic percolation problem)
- Inhomogeneous distribution of impurities
  - Phase separation (spinodal decomposition)
  - Layer-by-layer growth condition
    - Quasi one-dimensional structure
    - Superparmagnetic blocking phenomena

Magnetization curve

- Monte Carlo Simulation for Hysteresis loop

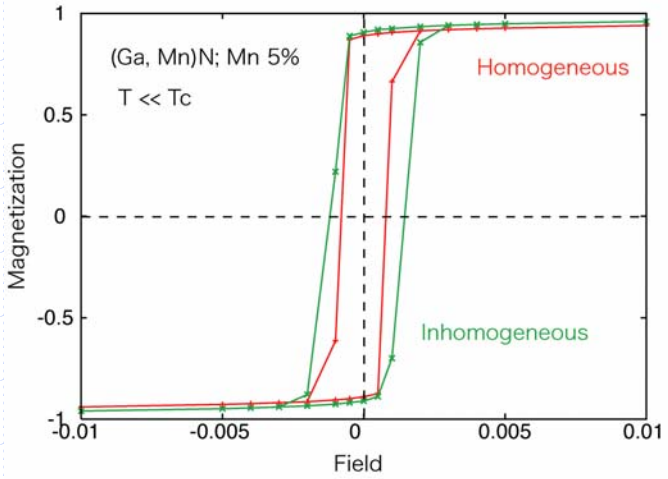

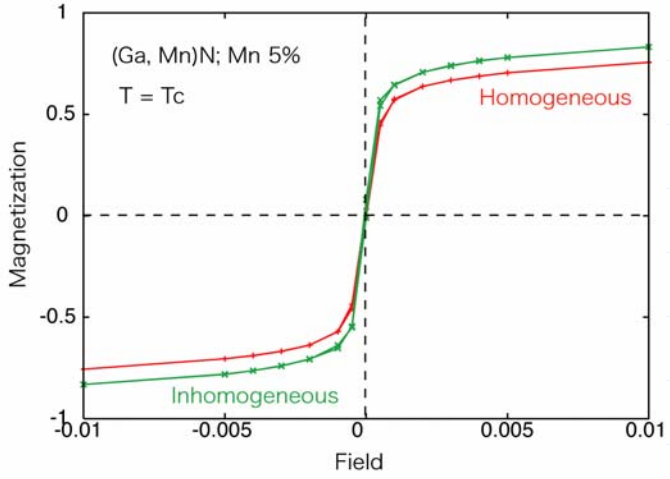

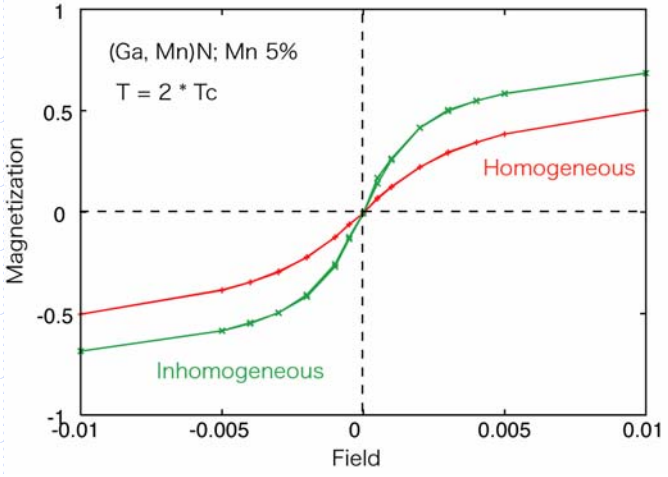

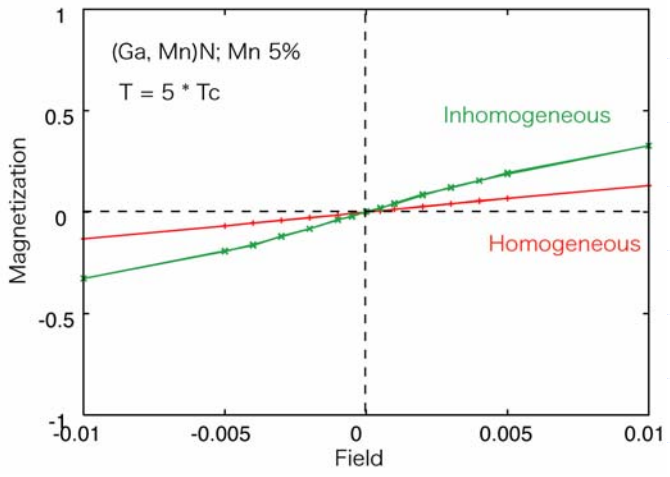

Super exchange interaction

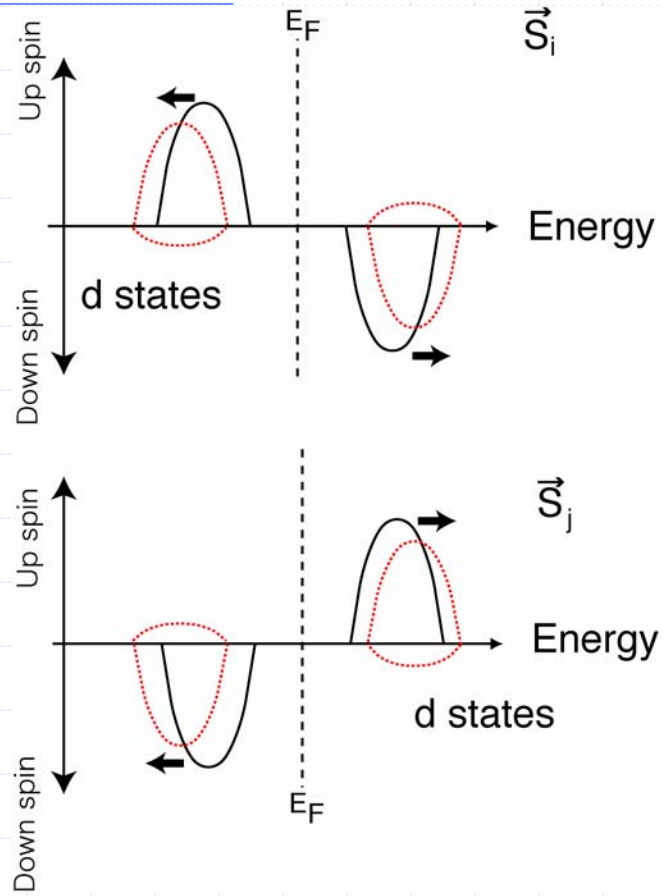

Anti-parallel configuration of two local magnetic moments

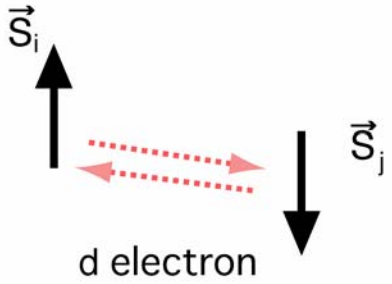

Anti-parallel configuration
→ Band energy gain by
the super-exchange interaction

Effects of spinodal decomposition on T_C of (Ga, Mn)As

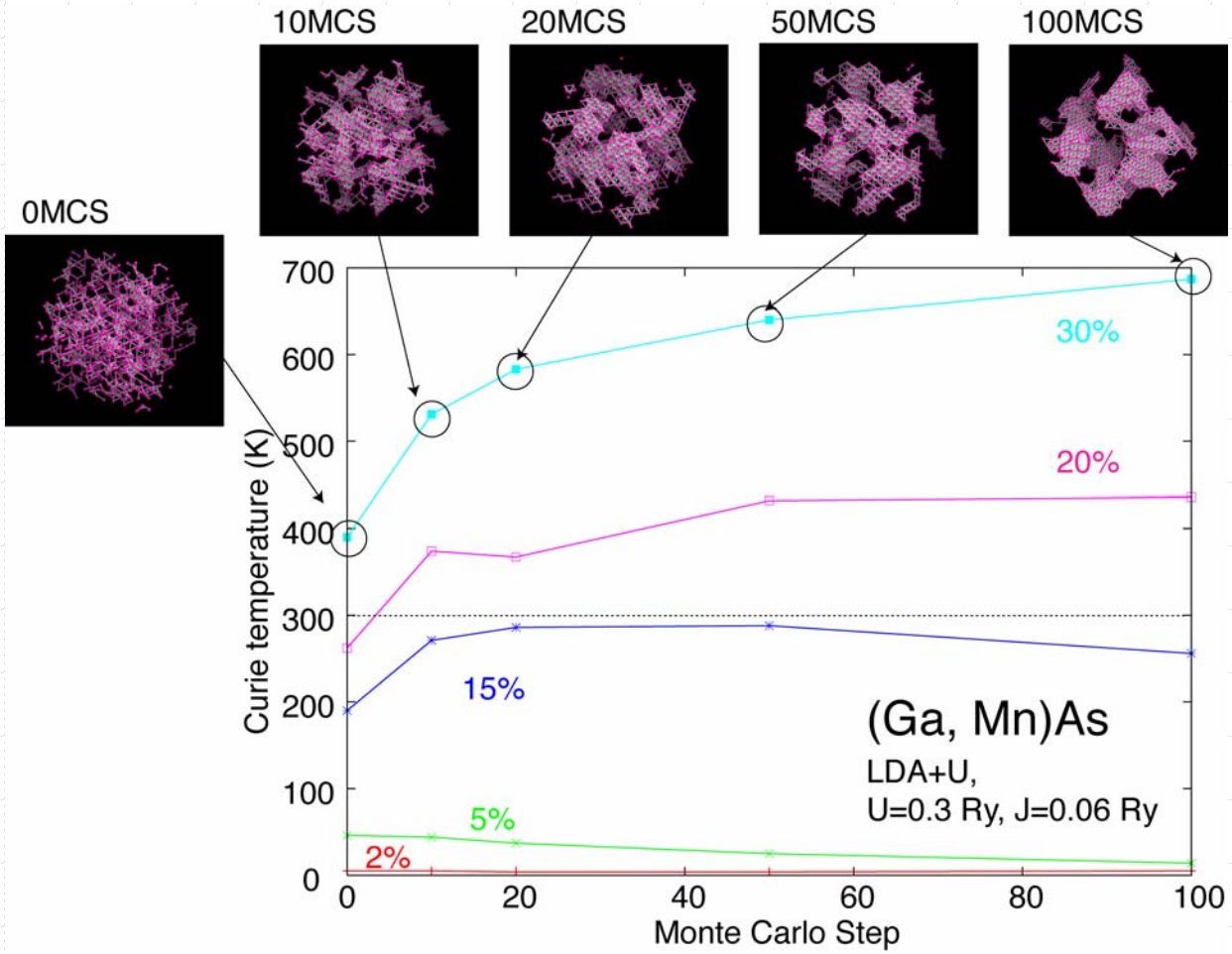

Systematic error of LDA

The LDA predicts occupied d-states at too high energy.

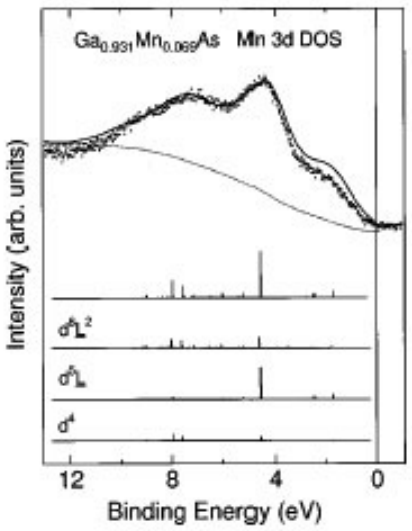

FIG. 3. Cluster-model analysis of the Mn 3*d* partial density of states assuming the Mn^{2+} valence state. The calculated spectrum is shown by a solid curve. The vertical bars are unbroadened spectra. In the bottom panel, the calculated spectrum is decomposed into d^4, $d^5\underline{L}$, and $d^6\underline{L}^2$ final-state components. The background is shown by a dotted curve. The dashed curve has been obtained by correcting for the overlapping As Auger emission (see Fig. 1).

Okabayashi et al., PRB 59 (1999) R2486

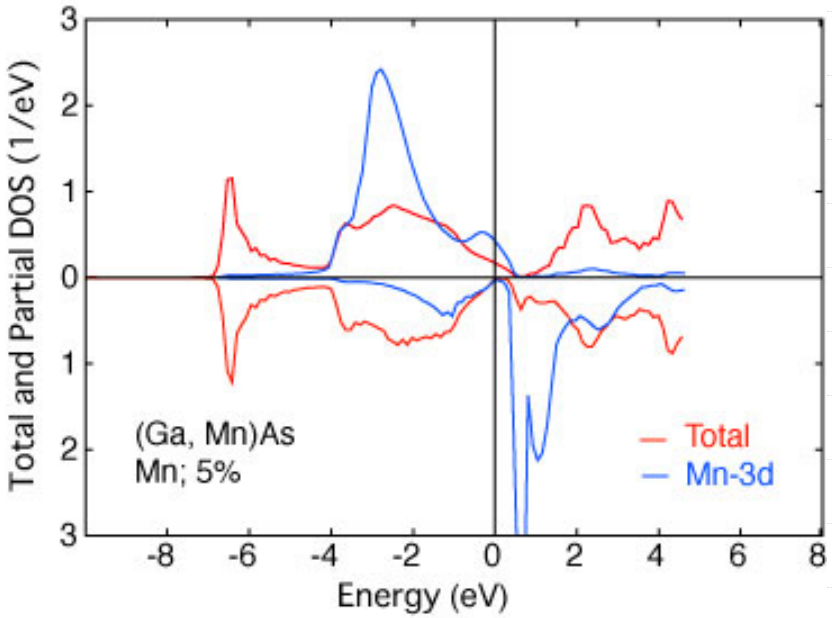

The ferromagnetism depends on the energetic position of d-states

→ LDA+U method

LDA+*U* method

In the LDA+*U*, Coulomb repulsion between electrons in localized state is treated by the Hubbard like procedure.

$$E_{LDA+U}[n^{\sigma}(r), \{n^{\sigma}_{m}\}] = E_{LDA}[n^{\sigma}(r)] + E_{U}[\{n^{\sigma}_{m}\}] - E_{dc}[\{n^{\sigma}_{m}\}]$$

$$E_{U}[\{n^{\sigma}_{m}\}] = (U/2)\sum_{\sigma}\sum_{m,m'} n^{\sigma}_{m} n^{-\sigma}_{m'} + (U-J)/2\sum_{\sigma}\sum_{m\neq m'} n^{\sigma}_{m} n^{\sigma}_{m'}$$

$$E_{dc}[\{n^{\sigma}_{m}\}] = (U/2)\,N(N-1) - (J/2)\sum_{\sigma} N^{\sigma}(N^{\sigma}-1)$$

$$V^{\sigma}_{LDA+U\,m}(r) = V^{\sigma}_{LDA}(r) - (U-J)\,(n^{\sigma}_{m} - 1/2)$$

$n^{\sigma}(r)$: electron density

n^{σ}_{m} : electron occupation

σ: spin m: orbital

$N^{\sigma} = \sum_{m} n^{\sigma}_{m}$ $N = \sum_{\sigma} N^{\sigma}$

U: Effective Coulomb interaction

J: Effective exchange interaction

Mn-doped III-V, U = 4 eV, J = 0.8 eV

Refs.: Anisimov et al., J. Phys. Cond. Matt. 9 (1997) 767, Solovyev et al., PRB 50 (1994) 16861, PRB 53 (1996) 7158

SIC calculation: ThM3.4C, M. Toyoda et al.

LDA+U calculations for (Ga, Mn)As

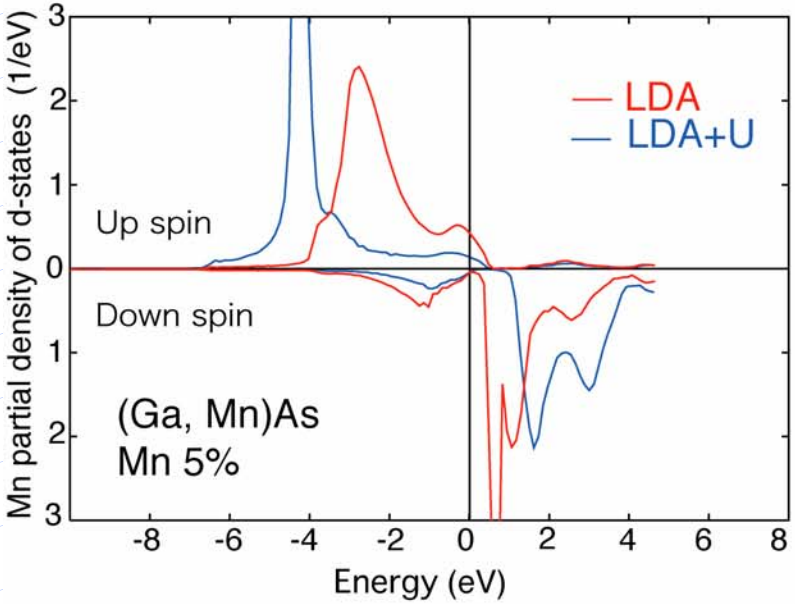

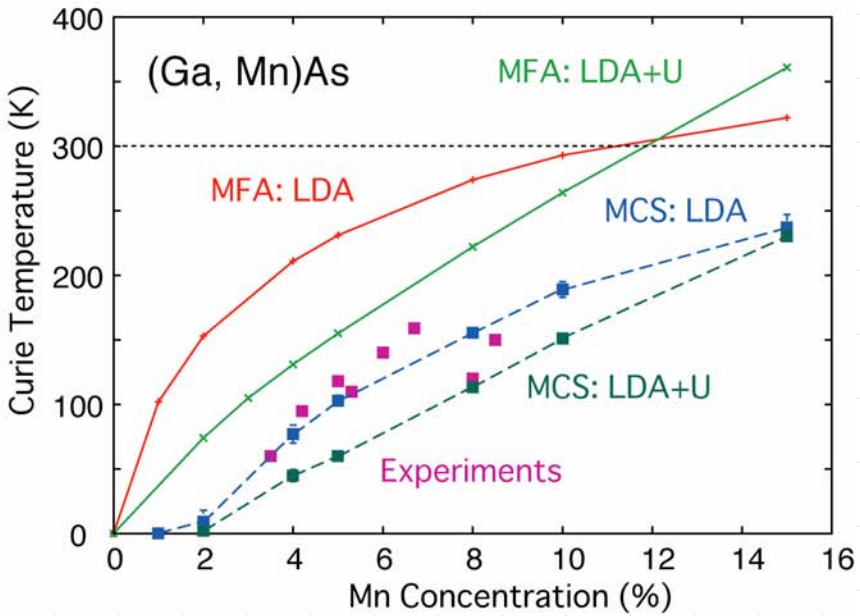

In LDA+U we find localized 3d states → p-d exchange

T_C is approximately proportional to Mn concentration.

LDA+U with MCS gives reasonable T_C values.

LDA+U calculations for (Ga, Mn)N

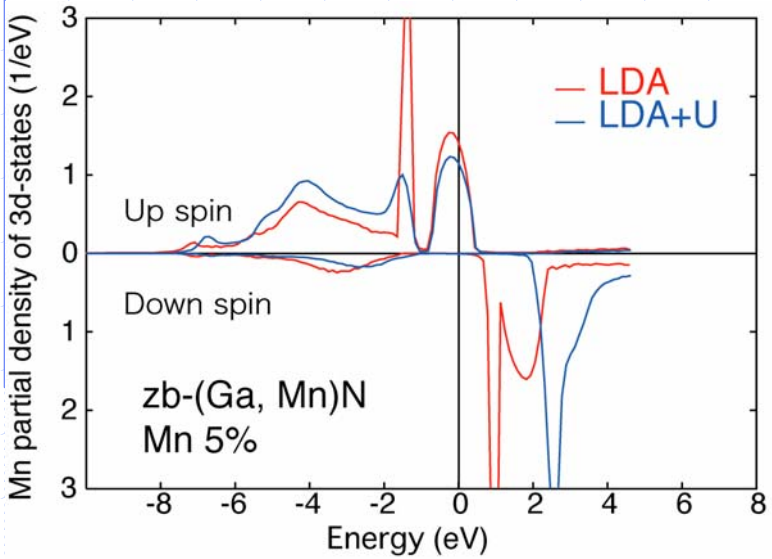

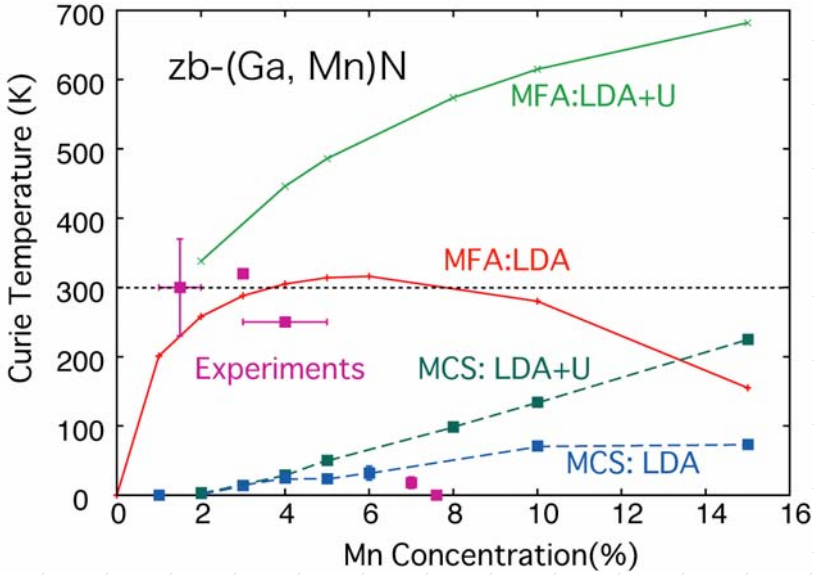

Around E_F,
the LDA+U predicts very similar electronic structure to the LDA.

Unoccupied d-states are shifted to higher energy.
→ anti-ferromagnetic super-exchange interaction is suppressed.

Self-Interaction correction:(Ga, Mn)As

- *M. Toyoda et al., 2006.*

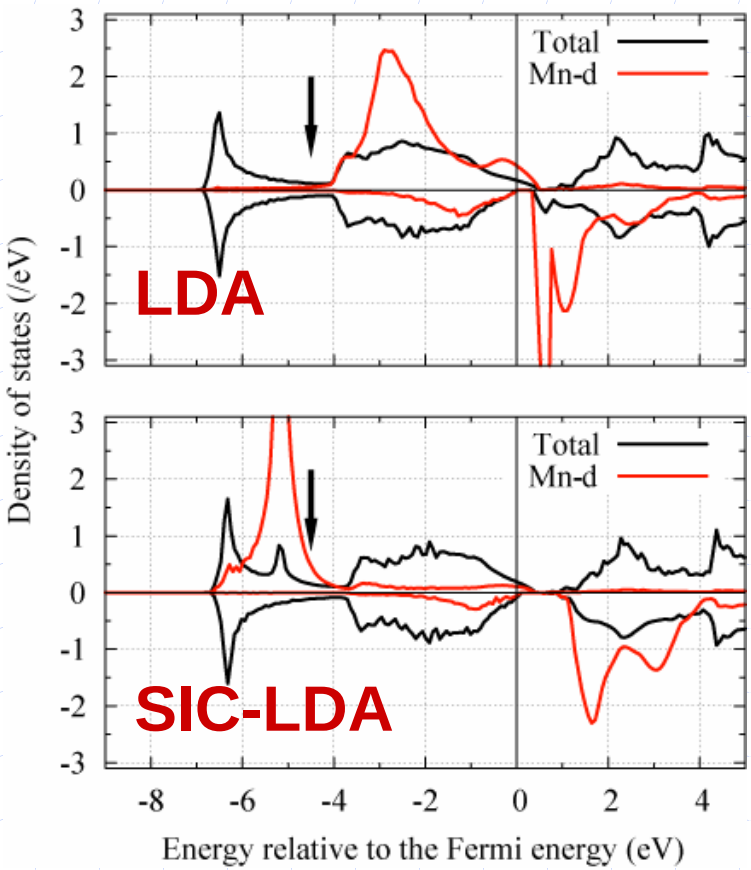

PES J. Okabatashi *et al.* (1999)

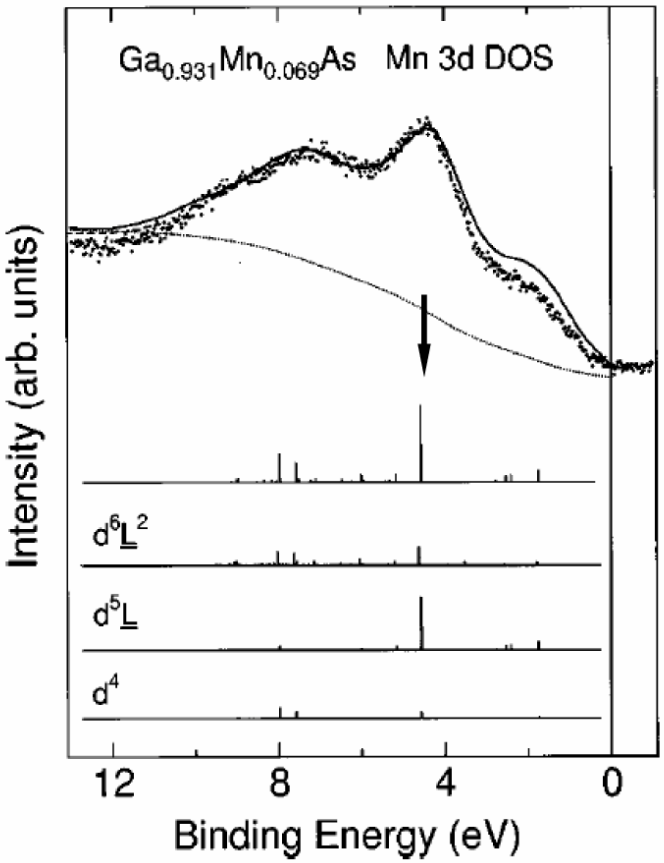

Zener's p-d exchange mechanism

Self-Interaction correction:(Ga, Mn)N

- *M. Toyoda et al., 2006.*

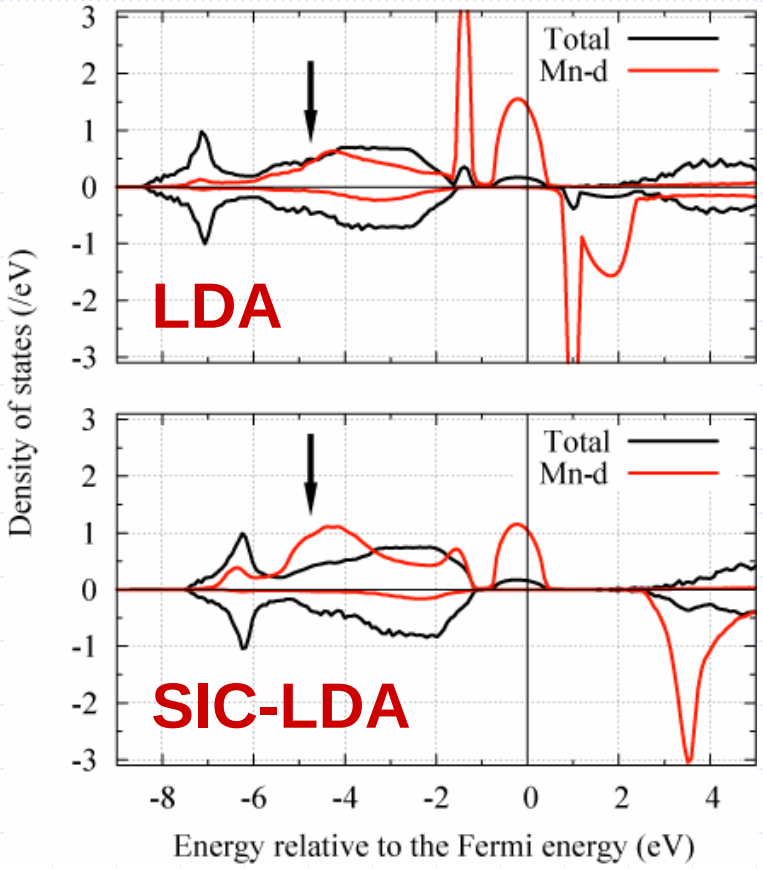

J. I. Hwang *et al*. (2005)

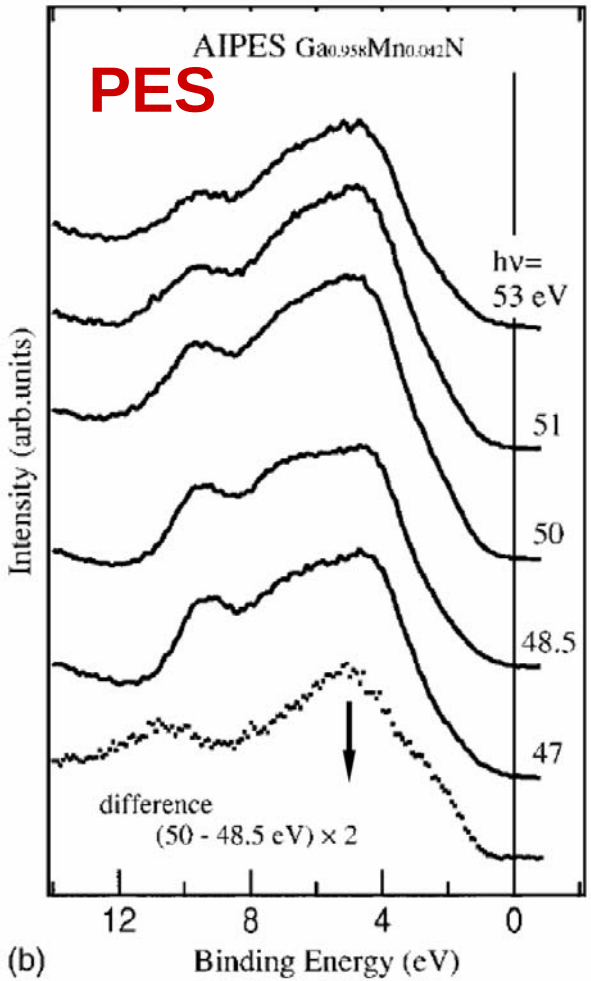

Zener's double exchange mechanism

Exchange interactions and T_C

Mn-PDOS

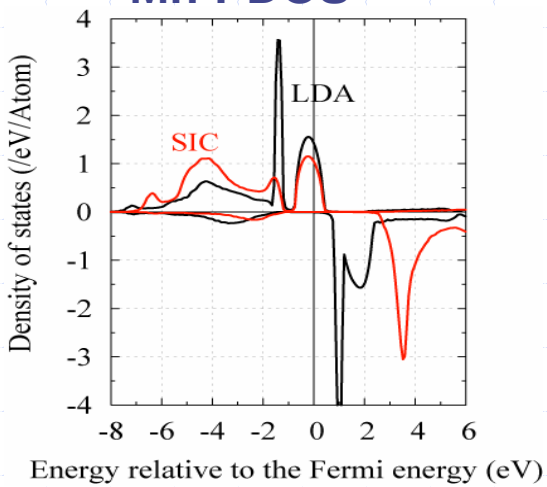

J_{ij} (x=0.05)

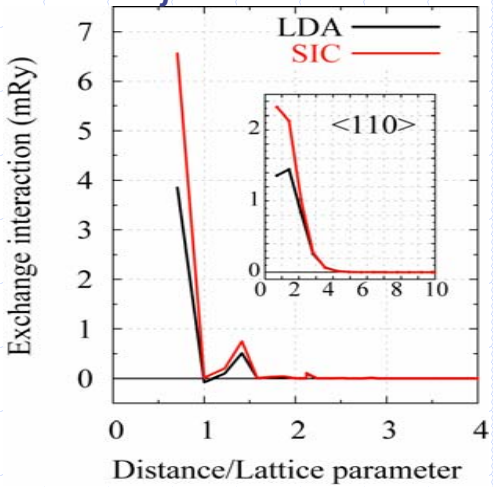

T_C (MFA)

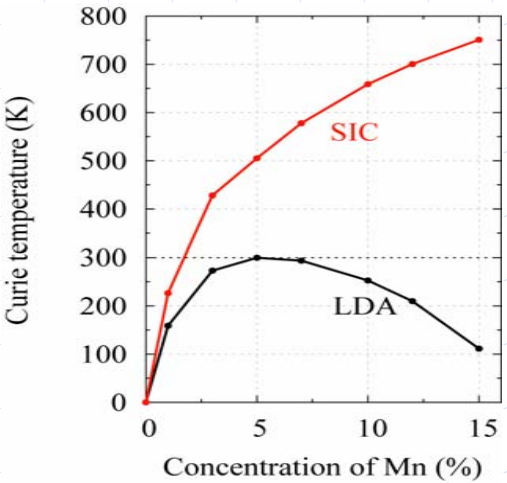

- Double-exchange-like
- DOS at E_F is smaller than in LDA.
- Exchange splitting is two times larger.
  -> Suppresses antiferromagnetic super-exchange Int.

Exchange interactions and T_C

Mn-PDOS

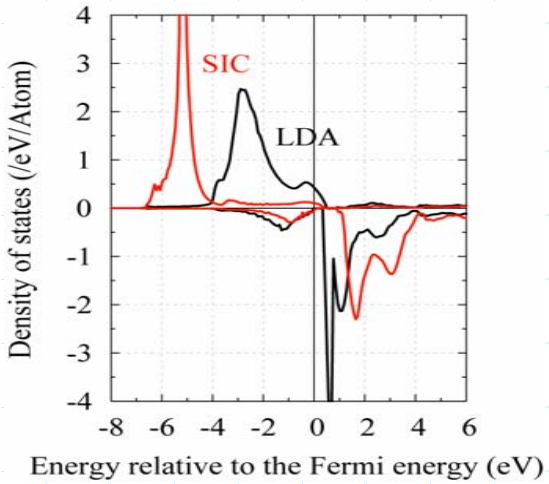

J_{ij} (x=0.10)

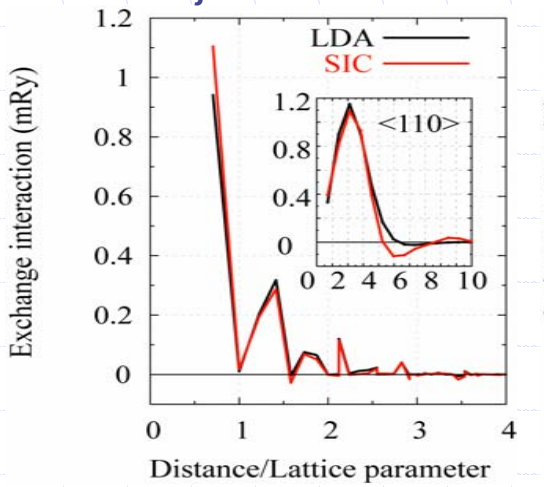

T_C (MFA)

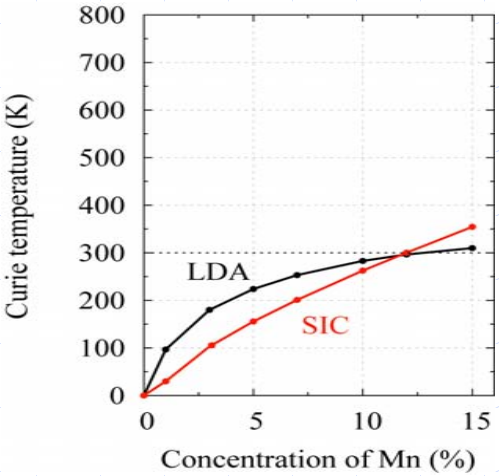

- *p-d*-exchange-like
- DOS at E_F is reduced.
- Long-range behavior of the exchange interactions.
  -> Enhances T_C in the diluted region (but not in MFA).

Self-Interaction correction:(Zn, Co)O

- *M. Toyoda et al., 2006.*

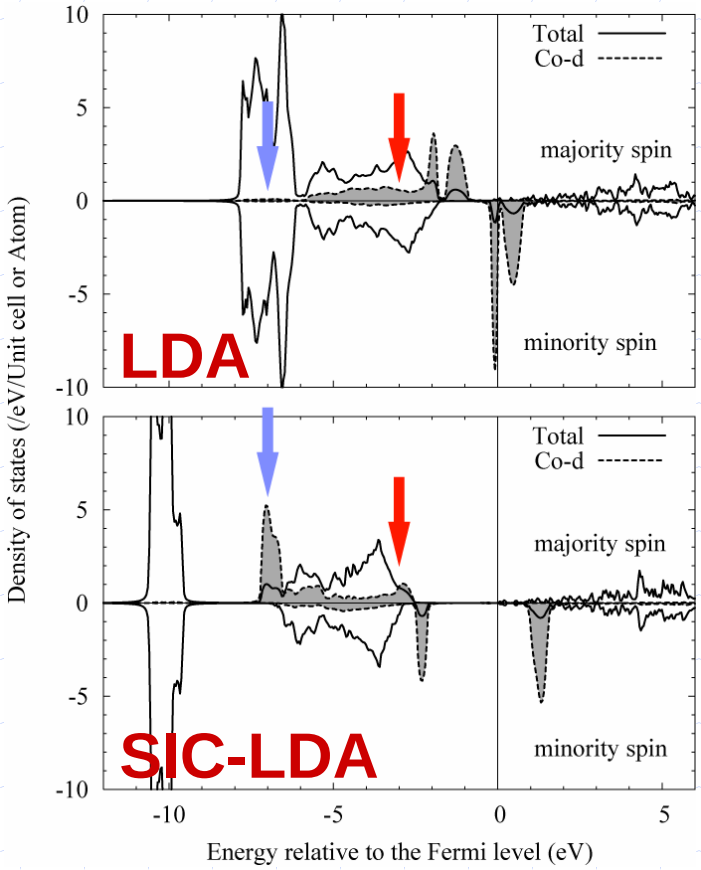

PES M. Kobayashi *et al.* (2005)

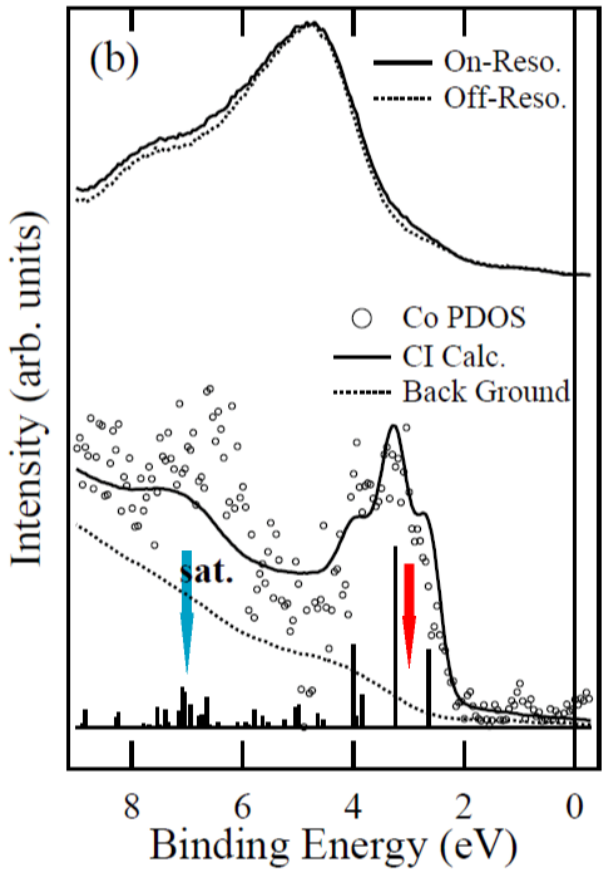

Weak ferromagnetic super-exchange mechanism